Analytica Chimica Acta 1147 (2021) 72–98

Contents lists available at ScienceDirect

Analytica Chimica Acta

journal homepage: www.elsevier.com/locate/aca

Review

Methodology and applications of elemental mapping by laser induced breakdown spectroscopy

A. Limbeck [a, *], L. Brunnbauer [a], H. Lohninger [a], P. Pořízka [b], P. Modlitbová [b], J. Kaiser [b], P. Janovszky [c, d], A. Kéri [c, d], G. Galbács [c, d]

[a] TU Wien, Institute of Chemical Technologies and Analytics, Technische Universität Wien, Getreidemarkt 9/164, 1060, Vienna, Austria
[b] Central European Institute of Technology (CEITEC) Brno University of Technology, Purkyňova 656/123, 612 00, Brno, Czech Republic
[c] Department of Inorganic and Analytical Chemistry, University of Szeged, Dóm Square 7, 6720, Szeged, Hungary
[d] Department of Materials Science, Interdisciplinary Excellence Centre, University of Szeged, Dugonics Square 13, 6720, Szeged, Hungary

HIGHLIGHTS

- Elemental imaging using LIBS.
- LIBS instrumentation - technical requirements for imaging applications.
- Strategies for advanced data processing.
- Selected applications in life sciences, geoscientific studies, cultural heritage studies and materials science.

GRAPHICAL ABSTRACT

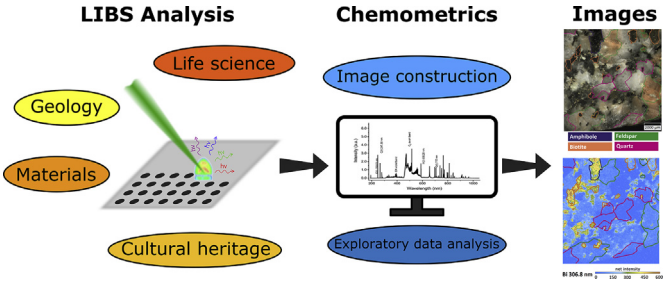

ARTICLE INFO

Article history:
Received 15 August 2020
Received in revised form
22 December 2020
Accepted 23 December 2020
Available online 30 December 2020

Keywords:
Laser induced breakdown spectroscopy
Elemental imaging
Technical requirements
Data processing
Application examples

ABSTRACT

In the last few years, LIBS has become an established technique for the assessment of elemental concentrations in various sample types. However, for many applications knowledge about the overall elemental composition is not sufficient. In addition, detailed information about the elemental distribution within a heterogeneous sample is needed. LIBS has become of great interest in elemental imaging studies, since this technique allows to associate the obtained elemental composition information with the spatial coordinates of the investigated sample. The possibility of simultaneous multi-elemental analysis of major, minor, and trace constituents in almost all types of solid materials with no or negligible sample preparation combined with a high speed of analysis are benefits which make LIBS especially attractive when compared to other elemental imaging techniques. The first part of this review is aimed at providing information about the instrumental requirements necessary for successful LIBS imaging measurements and points out and discusses state-of-the-art LIBS instrumentation and upcoming developments. The second part is dedicated to data processing and evaluation of LIBS imaging data. This chapter is focused on different approaches of multivariate data evaluation and chemometrics which can be used e.g. for classification but also for the quantification of obtained LIBS imaging data. In the final part, current literature of different LIBS imaging applications ranging from bioimaging, geoscientific and cultural heritage studies to the field of materials science is summarized and reviewed.

* Corresponding author.
E-mail address: andreas.limbeck@tuwien.ac.at (A. Limbeck).

https://doi.org/10.1016/j.aca.2020.12.054

Contents

1. Introduction

In the last century, atomic spectroscopy has been used for the analysis of almost all elements in a wide variety of sample types. Motivation for the measurement of metals as well as non-metals in natural but also industrial samples was driven by their influence on sample behaviour and properties. Moreover, knowledge about prevailing trace element levels also provides information about origin, formation or degradation of environmental or geological samples. For example, there is a clear need to determine the concentration of toxic elements in environmental, medical, or biological samples. The ability to catalyse environmental, biological or technological processes is another important reason for the assessment of metal concentrations prevailing in respective samples. Studies related to the determination of sample age or provenance benefit from the measurement of elemental ratios. However, the application of trace element analysis is not limited to earth sciences and life sciences only. In the last decades, the measurement of sample composition, additive levels and elemental impurities have become important in the field of materials science. Primary goal of these efforts is to maintain or even improve the intended chemical, physical or mechanical product properties.

For many years, simple analysis of bulk concentrations was sufficient for sample characterization. At the same time, it has also become customary in many research fields to collect information about the elemental distribution within the investigated samples. For example, the spatially resolved analysis of essential metals (such as Cu, Zn, Fe, Mn, Mg, and others), metalloids or non-metals (like S, P, N and halogens) in thin sections of biological tissues has become a subject of great interest in life science studies. Elemental maps are also of great importance in materials science, where typical applications include improvements in manufacturing and processing techniques such as deposition, diffusion or segregation processes, and coating or combustion procedures.

Thus, analytical techniques able to associate spatial coordinates to information on elemental composition are in high demand. Further requirements for appropriate methods include fast and simultaneous multi-elemental analysis of major, minor, and trace constituents, applicability for analysis of all kind of solid samples (conductive as well as non-conductive samples), no or negligible sample preparation, and no or minimal sample damage only. Since some types of environmental and biological, in particular medical samples are susceptible to vacuum, the method should work at ambient pressure to avoid unintended sample alterations.

In the last decades several analytical techniques capable of providing elemental imaging information have been employed for these purposes, including micro-X-Ray-Fluorescence-Analysis (μ-XRF), Electron Probe Micro Analysis (EPMA), Auger Electron Spectroscopy (AES), X-ray Photoelectron Spectroscopy (XPS), Secondary Ion Mass Spectroscopy (SIMS), Low Energy Ion Scattering (LEIS) and other synchrotron-based chemical imaging procedures [1]. Although each of these techniques has its own benefits (e.g. some are non-destructive (e.g. XRF), some are very surface sensitive (e.g. SIMS), and some provide also chemical information (e.g. XPS)), the method that complies with the requirements mentioned above to the largest extent is Laser Ablation-Inductively Coupled Plasma-Mass Spectrometry (LA-ICP-MS) [2]. Attributes that make this technique attractive for spatially resolved analysis of complex matrices such as geological, environmental, biological or technological samples are high sensitivity, wide linear dynamic range, fast

sample throughput, minimal sample preparation, minimal risk of sample contamination, and the ability to perform isotopic analyses. The steadily growing field of imaging applications include the characterization of advanced materials (e.g. metals, alloys, semiconductors, ceramic oxides, but also nitrides or carbides, composite materials) [3], the investigation of naturally occurring but also artificially introduced elements in hard and soft tissue material [4], but also geological samples such as rocks, minerals or meteorites [5].

Although LA-ICP-MS has become an established standard procedure for quantitative elemental mapping there still are three major limitations hampering the universal applicability of this method. Due to the transient nature of the signals produced in imaging experiments, the sequential operation mode of quadrupole and scanning sector field mass spectrometers (QMS and SFMS) does not permit the measurement of full mass spectra. Thus, a preliminary definition of the elements/isotopes of interest and therefore knowledge about sample composition is necessary prior to analysis. Moreover, in case of multi-element analysis the number of monitored m/z ratios is restricted when a certain degree in the quality of analysis (precision, accuracy, resolution) should be accomplished. A promising approach to overcome this limitation of QMS and SFMS instrumentation in imaging experiments is the use of a time of flight mass spectrometer (TOFMS), which provides access to full mass spectra and allows the identification of unknown sample constituents. However, independent from the applied type of mass spectrometer, LA-ICP-MS struggles with limitations in the sensitivity but also selectivity in the detection of most non-metals (such as S or P). The elements H, C, N and O, which are the major constituents of all organic compounds and thus all kinds of biological materials, and in addition also F for geological samples are not accessible at all. Finally, the aerosol generated during interaction of the focused laser beam with the sample must be transported from the ablation cell to the ICP-MS. Due to material losses in the transfer line, the efficiency of this transport step is always below 100%. Moreover, the wash out behaviour of the applied ablation cell determines the measurement time required for imaging experiments. With conventional ablation cells and QMS or SFMS instrumentation for samples in the mm x mm range, measurement times in the order of several hours are common. Combining the recently introduced rapid response cells with high repetition rate laser systems and ICP-TOFMS systems enables multi-elemental analysis of the same area in a fraction of that time. Nevertheless, even with these advanced ablation cells the repetition rates of commercial laser systems are not fully exploited.

Laser-induced breakdown spectroscopy (LIBS), another laser assisted technique used for elemental analysis, allows to overcome most of the main drawbacks of LA-ICP-MS. LIBS is also a micro-destructive method which requires practically no sample preparation, works under ambient pressure conditions and can be used equally well for bulk measurements and spatially resolved investigations [6,7]. In addition to these useful features, which were also fulfilled by LA-ICP-MS, LIBS offers some unique advantages that make this technique especially attractive for imaging applications. Although the first ground-breaking works were published in the late 1990s [8,9], a prerequisite for the development of a large number of imaging applications was the continuous improvement of applied laser systems, spectrometers and detection units in the last two decades.

In the meanwhile, LIBS has attracted increasing attention in the field of imaging [10] since it enables extremely fast imaging experiments with pixel acquisition rates in the kHz range [11] and a spatial resolution down to some μm [12] with valuable und numerous developments and applications published by the group of Vincent Motto-Ros [13]. The lack of need for the transport of ablated matter also eliminates carry-over and wash-out effects and transport efficiency is not an issue (even though with improved setups these effects are becoming less of an issue in LA-ICP-MS as transport efficiency improved from 40% in the beginning of ns-LA-ICP-MS to 80–90% in recent fs-LA-ICP-MS [14,15]).The ability to measure almost every element of the periodic table also including the elements H, C, N, O, and F which are not easily accessible by ICP-MS are further remarkable benefits of LIBS that are recognized in elemental imaging studies. Compared to alkali and earth alkali elements, which provide best detection limits, the sensitivity of non-metals is reduced. However, as these elements usually are main components this is not a limiting factor. In contrast to sequentially operating mass spectrometers, LIBS facilitates a simultaneous detection of the investigated wavelength range. Thus, with the collection of broadband spectra, no preliminary analyte selection is necessary and therefore, identification of prevailing elements can be done after the measurement. Additionally, statistical evaluation of broadband spectra is beneficial for sample classification. Moreover, LIBS spectra may also provide molecular information, which is useful especially in terms of polymer characterization and capabilities for stand-off analysis. Nevertheless, for some elements the sensitivity of LA-ICP-MS is still superior compared to LIBS enabling investigations with improved spatial resolution. Although the capabilities of LIBS for isotopic analysis have been demonstrated recently [16], LA-ICP-MS is still the method of choice for this special kind of analysis [17].

In Fig. 1, the basic concept of elemental mapping with LIBS is outlined. Within this review, a brief description of recent developments in instrumentation and technology is described. Different methodologies in terms of multivariate data processing, and calibration protocols for LIBS imaging are also discussed. The benefits of LIBS for spatially resolved analysis are presented by a selection of application examples from the fields of life sciences, geology and material sciences. Particular attention is paid to demonstrate the versatile character of LIBS, enabling the analysis of practically all kinds of solid samples without in-depth a priori knowledge of the sample composition. Finally, future prospects and potential applications of the technique are discussed.

2. Technical requirements

In order to be useful, LIBS imaging setups generally have to be designed and built specifically for the purposes of elemental imaging, due to a set of concomitant requirements that are usually demanded from conventional LIBS or LA-ICP-MS setups only separately. The primary reason for this is that not only the scanning laser ablation of the sample surface needs to be technically realized, but at the same time the plasma light also needs to be collected efficiently, therefore the optical and mechanical setup is more complicated than either in LIBS or LA-ICP-MS systems. The laser source, optical system, ablation chamber and the light detector all need to work concertedly to provide near ideal conditions for a fast, high-resolution, high-sensitivity LIBS imaging experiment. In the followings, we briefly overview the requirements set up by these conditions for the main components in the system. Readers interested in further technical details are kindly referred to reviews [13,18–22] and chapters in books [6,23–25] dedicated to LIBS instrumentation.

2.1. Laser source

The laser source has to be one that releases light pulses at a wavelength well absorbed by the sample material. The minimum pulse energy depends on the breakdown threshold (irradiance or power density needed to generate an LIB plasma) on the particular

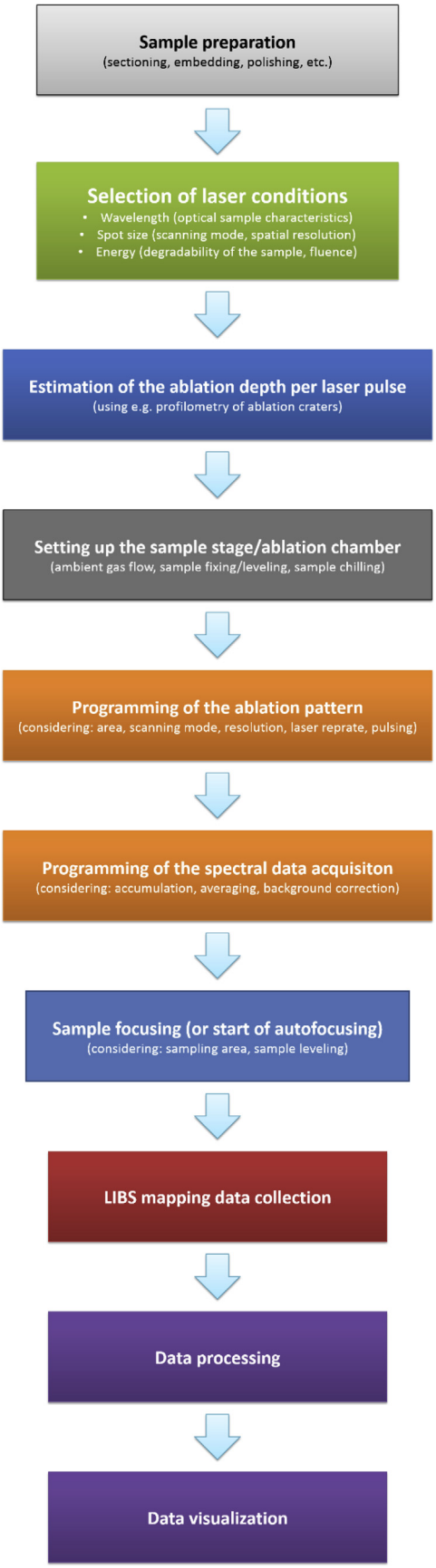

Fig. 1. A schematic flow chart of the preparatory and executive steps of 3D elemental mapping by LIBS.

sample. For most solids, GW/cm^2 irradiances are sufficient for this, which can already be achieved by using laser sources providing 10–100 mJ energy, 5–10 ns long pulses and a reasonable level of beam focusing. Since the spatial resolution of an imaging LIBS setup is always of primary importance, an advanced focusing optics is generally required anyway, which helps to keep the laser pulse energy requirement low. Good focusing, on the other hand, typically necessitates the laser source has a Gaussian intensity profile, as higher transversal modes can be less efficiently focused. It is also worth mentioning that flashlamp-pumped lasers often do not have the beam quality for tight focusing (e.g. 3–5 μm focal spots), unless they are built with an aperture-controlled resonator.

With regard to pulse energy, it is very important that the laser source provides an active control of the pulse energy and that the laser has ample reserve, in view of demanding samples with low absorbance. It should also be borne in mind that a high dynamic range (high contrast) attenuation of the primary laser beam (e.g. two orders of magnitude or more in energy) can usually only be achieved via the combination of at least two pulse energy control approaches (e.g. time-controlled active Q-switch, adjustable energy pumping source, rotatable polarizers, etc.) usually only available as options at a premium cost. We discuss further considerations related to both laser pulse energy and analytical spot size in the next section.

Meaningful laser wavelengths for LIBS purposes are typically in the UV or in the NIR range, especially for biological samples, where the selection should be based on the consideration of multiple factors. These include, but are not limited to the followings: *i)* the absorbance of the sample needs to be high at the chosen wavelength (to the benefit of sensitivity), *ii)* NIR wavelength, when combined with ns pulse duration, usually gives the best sensitivity in LIBS measurements, due to strong plasma heating which is proportional with λ^3, *iii)* UV wavelengths should always be preferred when spatial resolution is more important than sensitivity, as NIR laser ablation often generates strong thermal effects (charring) in the sample around the focal spot. However, wavelength is not an independent variable with laser sources. A certain laser type (active medium) will emit light at its characteristic fundamental wavelength and this can typically only be modified at a significant cost of pulse energy, also related to the regime of pulse duration (e.g. ns or fs). At present, most laser sources used in LIBS setups are still common solid-state lasers such as Nd:YAG or Nd:YLF. These lasers can offer high pulse energies only at their ca. 1064 nm fundamental wavelength and therefore other output wavelengths (532, 266 or 213 nm) are produced by employing nonlinear crystals, via the sum frequency generation technique, at a cost of 50–90% loss in pulse energy. Alternative laser sources are also available for LIBS use, such as excimer gas lasers, which can directly provide UV wavelengths (starting from 157 nm with an F_2 and up to 351 nm with a XeF medium), but they never really became widespread in analytical LIBS spectroscopy, due to their bulkiness and impracticality (e.g. frequent need for a refill of corrosive gases from gas tanks).

The selection of the laser source in terms of the pulse length regime (e.g. nanosecond(ns), picosecond(ps) or femtosecond(fs)) is also a subject of consideration. Apart from the significantly higher costs, fs pulses have been found to be advantageous from the point of view of a more stoichiometric ablation and therefore better analytical accuracy as well as a somewhat better spatial resolution (due to less debris around the crater caused by the smaller plasma plume). Please note though that smaller ablation spot size often also means smaller analytical LIBS signals. At the same time, ns pulses (assuming comparable irradiances) provide far better sensitivity, due to the higher mass of ablated material and more effective plasma heating/shielding. Thus, a fs laser source may only

be the better choice in an imaging LIBS setup, if the concentration of the analytes is high.

High repetition rate is a critical characteristic of laser sources suitable for LIBS imaging analysis, considering the large number of single point measurements to be performed during scanning. For example, a mapping task for an area of 1 cm^2 with a step size of 10 μm requires 1,000,000 measurements (without spot overlaps), which takes 13–27 h to complete with a laser operating only at the typical 10–20 Hz repetition rate. This measurement time is too long for many applications, where the use of lasers offering 1 kHz or higher repetition rates are required. In this respect, Q-switched diode pumped solid state (DPSS) lasers and fiber lasers, now becoming widely available commercially, have great potential. Typical Q-switched pulse energies of commercial lasers of these types are a few millijoules, although a tens of mJ fiber lasers and repetition rates in the hundreds of kHz range have already been reported [26]. Both DPSS and fiber lasers have superior beam quality, better stability and longer lifetime than conventional flashlamp-pumped Nd:YAG lasers, which convert to better spatial resolution, faster acquisition times and improved precision, thus at present these are the ideal, even if not yet widespread, laser sources for LIBS imaging analysis.

It also has to be added that while Ti:sapphire femtosecond laser sources are becoming more and more used in imaging LIBS setups due to their kHz-MHz range pulse repetition rates, high peak power and ultrashort pulses, they are actually not very good at producing single pulses [27]. They have difficulties with self-starting and stability, so they are very time-inefficient when it comes to single spot LIBS analysis (of course, these problems also affect fs LA systems). They are far more useful if trains of utrashort pulses need to be generated, which makes them most useful in continuous scan mode LIBS analysis (continuous line or area scans). For relevance of this in imaging LIBS, see section 2.5. On the other hand, DPSS lasers offer a good compromise between high repetition rate and reliable single-pulse operation; the achievable repetition rate with a DPSS is still quite high, typically some kHz.

Signal enhancement is always welcome in analytical spectroscopy, and LIBS elemental imaging is no exception. As is known from the literature, significant signal enhancement (up to ca. two orders of magnitude) can be achieved with the use of double-pulse or multi-pulse LIBS analysis (DP-LIBS and MP-LIBS) [19,28–33]. Although these approaches can be realized in several sophisticated optical configurations (e.g. with two lasers or a single laser, orthogonal/cross/colinear optical paths, delayed pulses, different pulse energy ratios, combination of IR/Vis/UV pulses etc.) when the analysis is carried out on a single spot, but the most practical one for LIBS elemental imaging is the colinear arrangement, which requires a special laser source that is capable of releasing a controlled burst of Q-switched pulses. Hence the use of the double-pulse approach in LIBS elemental mapping so far has been quite limited [34–37]. A drawback of the colinear DP-LIBS setup is that both pulses are ablative, which decreases the achievable depth resolution.

2.2. Laser focusing and light collection optics

Generally speaking, the optical setups used in LIBS instrumentation are quite diverse. Transmissive and reflective optical elements both in the laser beam focusing arm of the optical setup as well as in the light collection arm are equally used [24].

In an imaging setup, the beam guiding optics primarily should allow for a tight, variable spot-size focusing with a Gaussian intensity profile for the sake of high spatial resolution. Adequate focusing can principally be achieved by using a single “best form” lens, but for best results, a high numerical aperture lens (or a high damage threshold microscope objective) is needed, which has to be illuminated as uniformly as possible, so often a beam expander is also required to be incorporated in the optical path. For the sake of variable spot sizes, a zoom optics is needed, with multiple further optical elements. All optical elements in the focusing system need to be anti-reflection coated in order to maximize the pulse energy available on the sample surface and to minimize back-reflection of laser light into the laser source. If such reflections are not avoided they could deteriorate the performance of the laser, thereby inducing a loss of beam and pulse quality eventually leading to fluctuations in the LIBS signal. In more sophisticated setups, a Faraday isolator (rotator) can also be used to eliminate the back-propagation of laser beam. The smallest laser spot in a LIBS setup ever achieved was 450 nm [38].

In LIBS elemental imaging, the analytical spot size has to be chosen so that one also considers the area of the scan, the laser pulse energy available and the information content to be obtained. Choosing a smaller spot size means more information, which may be a necessity for a largely heterogenous sample with very small features to be resolved, but it also brings about a largely extended analysis time (with non-overlapping spots, halving the spot diameter makes the duration of the scan four times as long). This may not be practical for large area scans. A too small spot size may also decrease the analytical signal, thus the SNR of the obtained image may suffer for low concentration analytes. This is further complicated by the fact that very small spot sizes (ca. 40 μm or less) are often produced in LIBS systems by a size aperture (pinhole) setup, which wastes much of the cross section of the laser beam, and hence there usually is a significant pulse energy loss with these settings. Since the signal in LIBS, within the same pulse duration regime, is more or less proportional to both the amount of ablated matter and the fluence, the loss of analytical signal can be dramatic. The possibility to use very small analytical spot sizes is a definite advantage of LA-ICP-MS over LIBS in elemental imaging, which is due to the fact that in the former, the laser ablation is only used as a means of sample introduction and it is the ICP plasma that is responsible for signal generation, plus of course MS detection has very good sensitivity. This is also the reason why e.g. a ns laser LA-ICP-MS system can work well with as low as 1 mJ pulse energy and like 5 μm spot size, whereas with a similar laser source, LIBS struggles with spot sizes below some 10 μm in diameter and/or less than 10 mJ pulse energy. The much smaller fluences used in LA-ICP-MS also cause less damage to the sample around the ablation crater. The bottom line is that in most of the cases, it is advisable to choose the maximum spot size that is sufficient to resolve sample features and to pay attention to the laser pulse energy delivered to the sample.

In most LIBS setups, spherical beam guiding optical elements are used which produce a circular spot, however some analytical advantages have been reported to be associated with the use of cylindrical lenses producing rectangular spots (e.g. Refs. [39,40]). These may also be used in imaging setups in order to ablate more material (e.g. in square-shaped spots as opposed to circular spots) with a same scanning step resolution, thereby achieving higher signals. Another interesting optical approach for laser beam focusing is the incorporation of a microlens array described by Sturm in Ref. [41] in a LIBS imaging setup.

The depth of focus (defined as the distance from the point of minimum beam diameter after focus to the position at which the area of the beam has doubled, characterized by the Rayleigh range) increases linearly with the wavelength and with the square of the ratio of the focal length to the input beam diameter at the focusing lens [6]. The calculation gives about 4 mm depth of focus for typical conditions ($\lambda = 1064$ nm, $d = 12$ mm, $f = 120$ mm). In an imaging application, it means that for practical samples with minimal

surface corrugations (<1 mm), a reasonably small area of interest (e.g. 1 cm^2) and minimal tilting (the sample is affixed in a holder in a position that the area of interest on the surface is nearly horizontal), there is usually no need for auto-focusing during scanning, as the sample surface will not move out of the depth of focus, and therefore the irradiance on the sample surface will stay acceptably stable, which is a pre-requisite for accurate and precise elemental mapping. This is fortunate from the point of view of scanning speed, as auto-focus optomechanisms are usually not speedy enough to keep the pace with the rate of data collection needed (>kHz). Nevertheless, an auto-focus feature (based on e.g. time-of-flight measurements from a supporting beam of diode laser pulses or on a camera image) is very useful, because it makes the bringing of the starting spot into focus much easier. This additionally aids sample surface observation via a digital camera. It should also be mentioned that in contrast to surface measurements, the depth of focus requirements for depth-resolved analysis are more demanding. A small depth of focus is also preferred if the sample is a thin slice.

It should also be added that auto-focusing is typically only featured in commercial LIBS (and LA) instruments, but can not be expected to work equally well on all sample types. Typically, transparent samples give camera-based systems a hard time, and samples with strong specular reflection or very little scattering can easily mislead time-of-flight based systems. In addition to this, it can also cause similar problems if the optical characteristics of the sample show great variability within the mapped area.

A general optical alternative for rastering the beam across the sample surface instead of sample translation is steering the beam by a mirror system (driven by e.g. piezoelectric drives or galvo-scanners) and an *F*-theta lens. However, this arrangement is not practical in LIBS, because the emitted light from the plasma also needs to be collected and this would be very much complicated by the varying direction of the ablative beam during scanning.

The light collection optics should of course be optimized for maximum collection efficiency. First of all this means that the collection solid angle should be as large as possible/practical. Second, although the collection of the light emission by the plasma can be also effectuated from the side, but most light can be collected if the collection optics is uniaxial with the laser beam focusing optics („top view"). This is due to the fact, that breakdown plasmas always propagate outwards in the direction of the surface normal and in most setups, the direction of the laser beam is perpendicular to the sample surface. This arrangement however necessitates the optical separation of the forward propagating „monochromatic" laser light from the backward propagating plasma emission to be detected. The above requirements are best realized either by using a concave, collection mirror pierced for the focused laser beam or by using a telescope (e.g. Galilean) arrangement. The collected light, now collimated by the mirror, can then be focused onto the entrance slit (round or circular) of the spectrometer, preferentially using a reflective optical component again in order to avoid chromatic aberration. However ideal, this setup is rarely used in commercial LIBS imaging systems because the sample surface also needs to be observed with a high resolution digital camera prior to the measurement for the selection of the area of interest and sample documentation purposes. This can be done easiest if this third „observation beam" is collected uniaxially with the laser beam and the light collection is performed from the side on a different axis, at some cost of sensitivity. It should be mentioned that use of fiber optic cables to couple the emitted light into to the spectrometer is very practical from the point of view of system assembly, but it comes with significant further losses in sensitivity, especially in the UV range. This is caused by multiple problems associated with the process of coupling light into the fiber, limited transmission through the fiber and sub-optimal filling of the entrance slit with light, etc.

2.3. Ablation chamber and sample positioning

Employing an ablation chamber that is rarely used in conventional LIBS analytical measurements is hardly avoidable in imaging analysis. Although the use of an ablation chamber imposes certain limitations in sample size and shape, which necessitates some mechanical sample preparation, it is not a drawback since sample preparation is almost always involved with LIBS imaging anyway.

The ablation chamber also provides a possibility to perform plasma generation under an inert gas atmosphere with pressure and composition control. This can be beneficial with respect to *i)* enhancing the sensitivity by modifying plasma physics, *ii)* allowing the access of the VUV spectral region by purging oxygen and nitrogen from the optical path, *iii)* reducing gas-phase reactions in order to avoid some spectral interferences and *iv)* reducing the depositions and thermal effects on the sample surface thereby slightly improving spatial resolution. For example, it is well documented [42] that a decreased pressure (ca. 10 Torr) argon gas atmosphere generally gives the highest sensitivity in LIBS measurements, and the addition of He to the gas reduces the amount of debris produced during laser ablation, which can help increase the imaging resolution. The use of He as ambient gas is also beneficial when detecting nonmetallic elements, such as F and S, because the helium plasma has higher excitation potential than argon. Using a gas flow around the sample and in the chamber also helps to keep the window of the chamber clean of deposits, which would otherwise continuously decrease the transmission of the window, thereby leading to a decrease of the laser fluence reaching the sample surface and a decrease of the recorded emission signal. This is especially important in imaging applications, since a great number of laser pulses are delivered to the sample, so cleaning the chamber window after each few shots is not an option. As a rule of thumb, it is generally advisable to use a laser focusing optics in nanosecond LIBS at atmospheric pressure with a working distance of at least 10–20 mm in order to keep the optical elements at a safe distance from the ablation plume ejected from the sample surface and some of the gas reaction products - if the gas pressure is higher or a femtosecond laser source is used then the distance can be smaller, because these conditions produce a much smaller plasma. At the same time, this working distance will be higher if the ablation gas has a pressure significantly lower than atmospheric, the laser pulse energy is higher than usual or the samples vigorously get oxidized in the atmosphere, such as with polymers/organics, as the height of the plume will be larger. It also has to be considered that plasmas in argon are generally hotter and larger than those in helium, due to the higher thermal conductivity of the latter. It should also be noted that the purging of the ablation chamber with a gas flow ideally dictates to be performed at a volume rate which ensures the exchange of the gas between each laser shots. This, in turn, suggests that the volume of the chamber should be kept at a minimum – limited by the sample size and the chamber height (min. working distance), of course. The higher the laser repetition rate, the faster the gas exchange needs to be. The use of gas flow rates around 20 L/min are common.

A further device the use of which is crucial for a successful high repetition-rate scanning LIBS imaging application is a motorized, high-speed micropositioning two-axis (or if depth-resolved analysis is also planned, three-axis) translation stage that programmatically moves the sample under the focused laser beam. Needless to say that the linear resolution and the positional accuracy of these stages have to be in the sub-μm range, a value significantly smaller than the spatial resolution (analytical spot

size) aimed to be achieved, with a travel range that exceeds the lateral sample dimensions. In addition to this, the stage also needs to be very fast in *x*-*y* scanning speed, otherwise an ideally kHz-range repetition rate laser can not be exploited. As a numerical example, a fast precision translation stage with a 250 mm/s speed allows a 10 mm line to be scanned in 1/25 s. This speed can be exploited with a laser having 25 kHz repetition rate if a 10 μm spatial resolution is to be achieved. A Z-axis piezo translation stage, with a travel of, say, 500 μm is also necessary if depth-resolved analysis is planned (3D mapping). This limited travel range is sufficient for most such studies, considering the increasing difficulties in the efficient collection of light from an increasing depth ablation crater. It may also be added that the tilting of the sample surface (e.g. by employing a rotation stage working around either the *x* or *y* axis) can be used as an approach to enhance depth resolution [43]. Mounting the sample holder on a rotation stage also helps to ensure that the area of interest on the surface of the sample is horizontal for the scanning.

Considering the usual long time (several hours) needed for the imaging, the use of a thermostatable (cooling) sample holder should be considered in case of perishable (e.g. biological) samples. Without cooling, the microbiological degradation of the sample can cause analytical errors due to compositional changes (e.g. loss of volatiles) or phase transformations (e.g. liquefaction, thawing). Such sample holders are commercially available and are widely used in microscopy; the cooling is performed by a thermoelectric (TEC) device, supported by a recirculated fluid heat dissipation line.

The shape transformation or dimensional changes of the sample during the measurement time are also to be avoided. Flexible or mechanically not stable samples may not even be suitable for LIBS imaging. A common solution for fixing such samples is to embed them in a rigid polymer matrix, e.g. epoxy resin, and then cut the block at the right elevation to expose the desired cross section of the sample [44,45]. This approach has been long used in the field of microscopy and was taken over by the LA-ICP-MS and now by the LIBS imaging community. Another possibility to fix samples that are not rigid enough is to freeze them and keep them frozen during the whole measurement time by employing an above mentioned thermostable sample holder. It is worth mentioning though that local thawing of the sample and the production of water vapor under the action of the laser pulse is inevitable. This can complicate quantitative or 3D mapping measurements and the use of a dry purging gas becomes very important. Further details of the sample preparation of various applications can be found in section 4.

Last, but not least, the use of the ablation chamber is also preferred due to safety considerations – without an ablation chamber, the analysis of samples that impose chemical, radiological, or biological hazards is not advised.

2.4. Spectrometers and detectors

The dispersive optical arrangement of spectrometers used for elemental imaging is no different from regular LIBS analysis. The choice of the optical setup of the spectrometer is dictated by such features as spectral resolution, spectral coverage and sensitivity. Theoretically, no specific dispersive optical setup is preferred over the others in LIBS imaging, thus all major types of spectrometers (e.g. Czerny-Turner, Paschen-Runge, Echelle, etc.) are in fact used. It is mainly the type and characteristics of the photoelectric detector used what makes a difference in mapping.

Charge coupled devices (CCD) are common in LIBS. Linear or 2D CCD arrays, in an intensified (with a microchannel plate, MCP) or non-intensified form are mostly employed. Linear CCD arrays are mostly used in Czerny-Turner spectrometers, whereas CCD cameras can be found in Echelle spectrometers. Back-thinned, Si-based CCDs provide low noise levels and good sensitivity in the UV–Vis–NIR range and can be efficiently synchronized with at least μs triggering accuracy and μs - ms range integration times, suitable for gated LIBS detection. The spectral resolution and sensitivity achievable depend on the optical setup of the spectrometer as well as the pixel resolution of the CCD array. Compact spectrometers incorporating linear CCD array detectors (having 2048 or 3684 pixels) typically provide good sensitivity, but the combination of spectral resolution (0.05–0.1 nm) and spectral coverage (100–150 nm) they offer is sub-optimal for LIBS detection, hence are preferred in portable and cost-conscious instruments. Echelle spectrometers with megapixel CCD cameras on the other hand can provide good spectral resolution (ca. 10–30 p.m.) along with a more or less complete UV–Vis spectral coverage, at the expense of some sensitivity.

A common problem with scientific CCD and intensified CCD (iCCD) detectors is their strongly limited read-out speed (after exposition, the pixels are read out in a serial fashion, which takes a long time), typically in the 1–100 Hz range (1–100 frames per second). This obviously is a serious drawback in LIBS imaging, which gives best performance at frequencies two to three orders higher (10–100 kHz). At present, the best promise for this field is the development of complementary metal-oxide semiconductor (CMOS) photosensor arrays. These devices have advanced read-out electronics and some of them already offer Gpixel/s read-out speeds, allowing for a sustained > kHz acquisition at their full megapixel resolution. At this speed, the camera's record length also becomes an issue, as a high-speed camera is preferred to be able to store all the frames in its on-board memory buffer, thereby requiring multi-GB memory. These CMOS cameras are now commercially available, but they are quite expensive, and have not made their way into the mainstream spectrometers, partially because of their somewhat reduced sensitivity compared to CCDs. Nevertheless, they definitely represent the future of LIBS imaging detectors. It is also worth mentioning that using photoelectron multiplier (PMT) detectors in discrete wavelength spectrographs, such as the Paschen-Runge arrangement, is a viable option for high speed LIBS imaging, but it is only feasible in industrial setups which work with a pre-defined set of analytical lines [24].

2.5. Data collection modes

Further consideration should also be given to the planning of LIBS data collection; in other words, the measurement pattern or data collection mode. This is the approach the system will follow to scan the rectangular analytical area on the sample surface. Essentially, two basic approaches are possible: step scan and continuous scan. Whether the former or the latter is better for a given mapping application strongly depends on the laser, optical setup, ablation stage available in the system and on the analyte concentration.

In step scan mode, the sample stage moves step by step from one measurement spot to the next. In each location, a full feature LIBS measurement (with autofocusing, cleaning shots, signal averaging or accumulation, double-or multi-pulsing, etc., if needed) is performed and the stage only moves on when LIBS data collection is completed. Step scan mode is therefore very adaptive and can be employed in any LIBS system. The cost of this flexibility is the very slow speed of mapping, which - in addition to the above features – is further decreased by the necessity to accelerate, decelerate and letting to stabilize the stage between locations (which is also influenced by the weight of the sample). One would think that this limits the usefulness of step scan mode to small area elemental imaging, but in actuality, its ability to optically follow the change in surface elevation becomes increasingly useful when larger areas are to be scanned. Users of scanning LIBS setups with conventional nanosecond laser sources can benefit the most from the step scan

mode data collection.

In continuous scan mode, the stage is continuously moving, and the laser is continuously firing at a calculated relative rate that allows the achievement of the required lateral imaging resolution (distance of measurement spots). Obviously, only single-shot analysis is possible in continuous scan mode – there can be no cleaning shot, no signal averaging or accumulation to improve sensitivity, etc. Should the sample surface move out of focus while translating, practically there is also no possibility to re-focus the optics. On the plus side, continuous scan mode is faster than step scan, while it is also easy on the laser and the stage. The extra speed of continuous scan mode can be best exploited, if the laser has a very high repetition rate, the sample surface is very smooth and levelled, and the analyte concentration is relatively high. That is also the reason why scanning LIBS systems built around a femtosecond laser usually force the use of the continuous scan mode.

The overall organization of the ablation pattern is the same in both scan modes: the area of interest on the sample surface is covered by „horizontal" or „vertical" lines closely spaced next to each other. In order to minimize stage movement and hence the total scanning time, the stage steps to the next line position at the end of a line, following basically a serpentine sequence („progressive scan"). It is also worth mentioning that there is some dispute in the LIBS and LA-ICP-MS elemental imaging literature about that whether the overlapping or non-overlapping analytical spots, assuming the same spot size, are better to use in the scans. As usual, the truth is that both approaches have their pros and cons, which are again related to the characteristics of the given LIBS instrumentation. Logically, non-overlapping spots generate less carry-over of ablated material from one spot to the other (from one pixel to the other in the elemental image), therefore tend to produce a sharper map that is a better reproduction of a highly heterogeneous sample composition. At the same time, overlapping analytical spots are claimed to carry the advantage to produce super-resolution images, which means that by using post-processing of measurement data, an elemental map with higher resolution than that possible by adjacent, but non-overlapping spots can be produced. Since more debris around ablation craters is generated with nanosecond pulses, large spot sizes and high pulse energies, therefore it is not surprising that femtosecond LIBS systems promote the use of scanning with overlapping spots. An additional factor in these systems is that the repetition rate of the laser is often so high that sometimes the sample translation stage can not keep up the pace with it (especially at larger spot sizes), so the use of non-overlapping spots is not really an option. At the same time, conventional nanosecond laser-based systems, which are slower to scan, but provide more flexible and more sensitive LIBS mapping, can be used with or without spot overlap.

2.6. Two- and three-dimensional mapping

3D representations of elemental distributions in solid samples by LIBS is recently becoming more and more popular, as they provide a more informative and visually appealing illustration of data. Since LIBS is a (micro) destructive analytical technique, depth-resolved (3D) elemental mapping can only be carried out in a sequential way, that is by repeating 2D scans over and over the same sample area. In these experiments, the depth resolution is basically defined by the depth of the ablation craters generated by each laser shot (= the thickness of the layer removed by a 2D scan). The 2D images are then stacked in order to get a 3D image. Assessment of the depth resolution can be experimentally done by ablating layered reference materials. Counting the number of repeated laser shots (N) needed to penetrate a layer of known thickness (d) in a reference material, to be determined by monitoring the analytical signal from an analyte characteristic of either the topmost layer or the layer below, is the basis of the calculation (depth resolution = d/N). The depth resolution can be controlled mainly by the laser fluence, spot size and the angle of incidence for the laser beam [43].

Unfortunately, the actual realization of 3D LIBS mapping with a reliable depth resolution is quite complicated, especially for larger cumulative depths (many layers). The root of many of these complications are shared with 3D LA-ICP-MS mapping, so in order to conserve space here, the interested reader is kindly referred to the LA-ICP-MS imaging literature (e.g. Refs. [4,46]). These complications include, among others, the followings: *i)* mapping via laser ablation leaves behind a roughened (crated- and debris-ridden) surface, where the overall height of corrugations (depth) can not be well defined (continuous scanning also suffers from the same problem, when the whole analytical area is considered); *ii)* the depth increase caused by each laser pulse becomes less and less as the ablation depth increases; *iii)* after each 2D scan, the sample stage is supposed to move the sample up into the depth of field (DOF) of the focused laser beam again, but it will not be easy for the autofocusing optical subsystem (either camera-based or time-of-flight distance measurement-based) to control this movement, with a roughened up analytical area (of course, the extent of these difficulties also depend on the optical system and the intended depth resolution); *iv)* the debris left behind in each area scan (it can not be completely avoided) will spread the ablated matter over onto adjacent craters, thereby „smearing" adjacent pixels of the elemental map generated (this effect will intensify with the ablation of each layer); *v)* signals collected during the depth-resolved elemental imaging of porous materials (e.g. polymers or layers with discontinuities) will also have contributions from underlying layers of the material, thus the interface between layers can not be correctly detected; *vi)* for heterogenous samples, the ablation rate can also vary from point to point. One consequence of these and other related complications is that only a few depth layers can be mapped – or in other words, the depth of the mapped sample volume should be practically much smaller than the side length of the surface area (unless very small areas are scanned).

2.7. Stand-off mapping

Stand-off LIBS analysis in single spots has been successfully demonstrated in the literature by many times, in several applications ranging from laboratory experiments to industrial monitoring, or from underwater archeology to planetary expeditions [19,22,47]. The tasks of focusing the laser beam over a distance and collecting the plasma emission with a telescopic optical system can be practically solved, as is also illustrated by the availability of several commercial LIBS measurement systems (see e.g. company websites of Applied Photonics, CEITEC and others). It is also known that the use of fs lasers in this scenario is especially advantageous, as the self-focusing filamentation of these laser beams make it easier to maintain the high fluence needed for plasma generation on the sample surface from a distance [27]. Rastering a laser beam over an analytical area is also a routine optical task, which can be done e.g. by galvo scanners. This can lead one to the conclusion that it is relatively straightforward to build a stand-off LIBS elemental mapping setup with analytical features comparable to those working in the lab.

In reality, there are several obstacles that need to be tackled for a successful stand-off LIBS imaging. First the sensitivity of a stand-off LIBS system is inherently much lower than that of conventional LIBS setups due to the very small light collection solid angle. If trace elemental mapping is to be attempted then this has to be compensated for by, e.g. increasing the size of the analytical spot

while keeping the laser fluence at the same level, but this will seriously deteriorate the spatial resolution of the elemental map and may need a very powerful laser. Another possibility is to use a non-conventional spectrometer which is far more sensitive – for example, interferometric spectrometers, such as the spatial heterodyne spectrometer (SHS) can boost sensitivity by a factor of 100 [48–50]. Second, any temporal or spatial fluctuations in the medium in which the laser pulse has to travel from the source to the sample will have an influence on the intensity or direction of the beam during scanning which can compromise the spatial resolution and the intensity of the elemental map obtained. Third, in stand-off analytical scenario, a clear view of the sample surface is needed, which typically also means that the sample is exposed to the influence of any environmental contaminations during the scanning time, which can easily be hours, and this may introduce spikes, glitches in the map recorded.

Table 1 offers an overview regarding commonly used laser parameters and instrumentation in various LIBS imaging applications.

3. Data processing of LIBS imaging

The following discussion applies to full LIBS spectra and not only selected wavelengths, as this is sometimes done to speed up the measuring process and to reduce memory requirements. While there is plenty of literature dealing with simple univariate approaches (an overview is given, for example, by Jolivet et al. [13] and by Zhang et al. [51]) we deliberately focus on multivariate methods which can clearly outperform conventional approaches both in accuracy and flexibility.

3.1. Conversion of 3D data

LIBS images form, as any other type of hyperspectral images, three-dimensional data sets (two spatial dimensions and one spectral dimension). However, most readily available chemometric methods work on two-dimensional data matrices which makes it necessary to convert the measured 3D data space into a 2D data space before applying multivariate statistical methods. The 3D to 2D conversion is done by means of serialisation: each pixel of the image is considered to be an independent sample [52]. Thus, all pixels of the image are arranged into a two-dimensional array, where the rows are the pixels and the columns are the intensities (Fig. 2). Of course, after applying the statistical toolset the processed data has to be transformed back to image coordinates. This way it is possible to present the processed data as images showing specific aspects of the original data.

There is one drawback to this approach: this transformation ignores the spatial relationship between neighbouring pixels because each pixel is treated independently. Thus special methods should be used to exploit spatial relationship as well. This can be done by performing, for example, texture analysis in parallel to hyperspectral analysis as it has been done with images obtained from the Mars rover Curiosity [53].

3.2. Automatic selection of spectral peaks

Given that full LIBS spectra have typically thousands of spectral peaks an automatic selection of peaks is more or less mandatory. Actually, one may have two goals when selecting spectral peaks: *i)* finding and identifying *all* peaks and *ii)* finding the important peaks which allows to solve a particular problem. Whether option *i)* or *ii)* is the best way to go depends on the type of the subsequent analysis. In the case of exploratory analysis one should use all peaks in order to avoid loss of information, and in the case of a specific classification task, for example, one wants to identify only those peaks which have the greatest contribution to the classification. In general, one should first identify all available peaks and use this set of peaks as the starting point for the next steps of the analysis. There are several methods, for example random forests, which provide an intrinsic selection of proper wavelengths.

One way to automatically select spectral peaks is to identify them by a method called image features assisted line selection (IFALS) [54]. IFALS performs a geometric analysis of the spectral curve which allows for detecting peaks in the spectral line. This method comes from machine vision where it is used in motion detection [55].

Another method is to correlate the spectral line with a small template peak while shifting the template peak along the spectral axis. Maxima of the correlation indicate the position of a spectral peak. This method is sensitive to peak width and may require running the algorithm several times with adjusted widths of the template peak. While the IFALS method is in general faster it exhibits some problems if peaks are driven into saturation (peaks are cut off and show a flat top). The correlation method is more reliable in such cases, given that the template width approximately matches the peak width of saturated peaks.

3.3. Pre-processing and scaling of the spectra

Depending on the multivariate methods applied during data analysis the scaling of spectra may be necessary or must not be applied at all [56,57]. In general, methods based on distances, such as hierarchical cluster analysis, must not be preceded by scaling operations, and methods based on variances, such as Principal Component Analysis (PCA), can use scaled data and might benefit from it.

The most often used scaling types are mean-centering and standardization. Mean-centering calculates the mean of the intensities of each wavelength and subtracts it from the corresponding intensities. This shifts the entire data cloud to the origin. Standardization mean-centers the data and then divides the individual variables by their respective standard deviation. Thus, the extent of the data space becomes comparable along all axes. Please note that standardization destroys the spectral correlation to some extent, a fact which might become important when a particular method requires the preservation of the spectral correlation (i.e. when applying an internal standard).

In many cases there is no clear rule when to apply which type of scaling. Thus, it is recommended to experiment with all three types of scaling (no scaling, mean-centering and standardization) to find out which approach fits best.

Pre-processing in LIBS-based hyperspectral imaging is straightforward and comparatively simple. Basically, two methods are often to be used: *i)* scaling the spectra to take care of varying experimental conditions during the measurement (which may take several hours if the image has a high spatial resolution). This can be easily achieved by, for example depositing a thin uniform layer of gold on the sample and using several of the gold lines as an internal standard to correct the spectra [58]; *ii)* In many situations, especially when the concentration of a particular analyte is low, noise acquired during the measurement of the data can become a considerable problem. Although many applications simply use spatial down-sampling approaches to reduce the spectral noise this approach is not recommended because information is destroyed (i.e. the spatial resolution decreases).

One of the methods to reduce noise without decreasing spatial resolution is to perform a principal component analysis, remove the components exhibiting low eigenvalues and back-transform the reduced set of principal components to the original data space. In this way it is possible to remove noise from the image data.

Table 1
Overview of used LIBS instrumentation in various imaging applications. Application fields LS: Life science, GS: Geoscientific studies, CH: Cultural heritage studies, MS: Materials science.

Laser Wavelength (nm)	Laser energy (mJ)	Pulse duration	Lateral Resolution (μm)	Detected Wavelength (nm)	Reference number
532/1064	30/80	ns	100	200–975	[37]
1064	–	ns	15	250–330	[52]
266	–	ns	100	185–1048	[83]
266	3.8	ns	100	185–1048	[84]
266	21.5	ns	40	185–1048	[113]
266	0.8	ns	25	315–350	[114]
266	15	ns	100	185–1040	[115]
532	–	ns	–	200-510/200-900	[116]
532	20	ns	100	270–1000	[118]
266	20	ns	150	187–1041	[119]
266/1064	10/100	ns	200	–	[120]
266	15	ns	–	–	[121]
1064	160	ns	100	200–1100	[122]
1064	90	ns	75	200–850	[123]
532	20	ns	100	240–940	[124]
532/1064	60/60	ns	–	240–860	[125]
1064	0.5	ns	12	315–345	[127]
1064	15	ns	100	315–350	[128]
1064	5	ns	100	286–320	[129]
1064	0.5	ns	40	315–350	[131]
1064	5	ns	–	282–317	[133]
1064	2	ns	50	190–230	[134]
532	–	ns	500	253–617	[137]
266/1064	10/90	ns	150	–	[138]
1064	70	ns		190–970	[139]
266	10	ns	500	–	[143]
532	20	ns	300	200–975	[144]
1064	35	ns	700	200–600	[145]
1064	0.5	ns	50	250-480/620-950	[146]
1064	–	ns	10	245-310/400-420	[147]
266	18	ns	100	240–800	[148]
1064	10	ns	90	270–330	[149]
1064	0.6	ns	15	190-230/250-335	[150]
1064	1	ns	10	–	[151]
1064	0.6	ns	10	150–250	[152]
213	–	ns	85	668–708	[153]
213	6	ns	50	284–333	[154]
1064	60	ns	250	220–800	[155]
266	6.75	ns	50	185–1050	[156]
1064/1064	50/10	ns	60	198-710/284-966	[157]
1064	1	ns	50	252–371	[158]
355	170	ns	700	360–800	[163]
355	170	ns	–	280–800	[164]
1064	50	ns	300000	240–340	[165]
1064	1.5	ns	8	200–1000	[166]
266	2.5	ns	80	180–1050	[167]
1064/1064	5.4/8.7	ns	20	190–900	[168]
1064	2	ns	6	130–777	[171]
1064	–	ns	100	186–1040	[172]
400	0.2	fs	6	–	[173]
1064	10	ns	30	190–210	[174]
532		ns	–	209-225/335-345	[175]
1064	0.6	ns	15	338–362	[176]
1064	1	ns	30	150–255	[177]
343	0.16	fs	75	390-403/452-500	[178]
266	8.4	ns	40	185–1048	[179]
532	20	ns	–	200–895	[180]
1064	3	ns	80	747–941	[181]
1064	65	Ns	0.67	200–980	[182]
532	120	Ns	1500	200–980	[183]
266	2	Ns	10	364–398	[184]
1064	100	Ns	800	258-289/446-463	[185]
266	2	Ns	25	–	[186]
266	2	Ns	25	272–775	[187]
532	2.9	Ns	130	187–1045	[188]
-	0.6	Ns	12	310–350	[189]

However, this approach has a big drawback: the principal components are sorted according to decreasing variance which might lead to the removal of valuable image information if the removed components contain useful information.

An alternative approach which uses basically the same idea but exploits a different weighting of the information content is maximum noise fraction (MNF) transform [59]. The basic idea behind MNF transform is to rotate the data space in a way that the

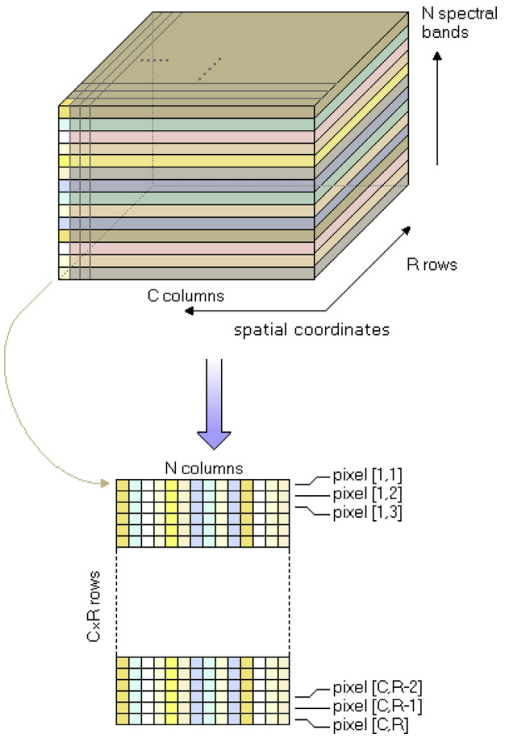

Fig. 2. The conversion from the 3D image space to the 2D analysis space.

signal to noise ratio is maximized along the new axis (instead of the variance in the case of PCA). The only problem with MNF is that it is necessary to correctly estimate the covariance structure of the noise. MNF transform works quite well if the structure of the noise is estimated correctly. If it is impossible or difficult to create a correct estimate of the noise structure, the results will be poor, resulting in artefacts which may hamper the following analysis of the image.

3.4. Data analysis

3.4.1. Exploratory analysis

Exploratory data analysis is a valuable toolset when just starting to get into the analysis of a largely unknown sample. All these methods are governed by the principle that the high-dimensional data space is projected onto a two dimensional space (i.e. the computer screen) in a way that the information contained in the high-dimensional data is largely conserved. The following section shortly discusses the most prominent methods used for exploratory purposes and gives some hints on introductory literature as well as on applications:

3.4.1.1. Principal component analysis (PCA) [37,52,60,61]. The basic idea of PCA [62] is the rotation of the *p*-dimensional coordinate system to achieve uncorrelated axes which show a maximum of variance of the data space. The maximizing of the variance is governed by the idea that the information content is proportional to the variance in a certain direction of the data space. This way it is possible to sort the resulting new (rotated) axes according to their information content. Without going into the mathematics of the PCA we can assume the first few components will show a big part of all available information. And indeed, PCA can be easily used to find spectrally similar regions of an image by looking at the score plots (Fig. 3).

3.4.1.2. Hierarchical cluster analysis (HCA). Hierarchical Cluster Analysis [64,65] generates dendrograms which depict the distances between individual spectra. The fundamental idea is that similar spectra show small distances in the *p*-dimensional data space and thus form clusters of neighbouring points in this space. There are several ways to create dendrograms which differ in the weighting of the inter-cluster vs. the intra-cluster distances (controlled by the Lance-Williams equation [66]). The resulting dendrograms can be quite different, not all of them being easy to interpret. A notably good choice is Ward's approach (which can also be covered by the Lance-Williams equation) [67]. The resulting dendrogram can be used to assign class numbers to all the spectra according to their mutual distance, thus effectively colouring chemically similar regions of a sample.

3.4.1.3. Similarity maps. Similarity maps [68,69] are basically maps which depict the spectral similarity of all spectra of an image to a reference spectrum. The reference spectrum may either be taken from the acquired image data or from a database. Thus, the user can quickly identify regions which are similar to a particular spot of the sample or similar to selected database spectrum. The spectral similarity can either be based on some kind of correlation or on some kind of spectral distance. Typical similarity measures are the Euclidean distance, the Mahalanobis distance [70], the Pearson's correlation coefficient, the spectral angle mapper [71] or spectral information divergence [72] (Fig. 4).

3.4.1.4. Vertex component analysis (VCA). The idea behind VCA is to resolve a linear mixture model in order to identify pure component spectra [73]. VCA is commonly used in endmember detection in geology and mineralogy and assumes that there are pure spectra of the searched components in the image. VCA operates on the raw data and its speed depends on the dimensionality of the data space. This automatically slows down VCA for full-scale LIBS spectra as these spectra have typical lengths of more than 10.000 intensity values.

3.4.1.5. Self-organizing maps (SOM). SOMs is a non-linear projection method which tries to segment images while maintaining topological relationships [74]. Thus, SOMs lend themselves to be used in imaging applications. SOMs have the advantage that the expected number of clusters has to be known (as opposed to, for example, *k*-means clustering).

Several applications have been published using SOMs. For example, Pagnotta et al. use SOMs to segment LIBS images of mortars [75], or Tang et al. use SOMs and *k*-means clustering to classify polymers [76] whereas Klus et al. used SOMs to study U-Zr-Ti-Nb in sandstone [77].

3.4.2. Classification

Classification methods are used when one wants to predict and assign the type of an unknown material. Classifiers are not "instant methods", in fact they have to be trained by known correct samples. This implies additional efforts, especially as far as the correctness of the training data is concerned (because wrongly labelled training data automatically lead to poor classification results). However, if the training sample is correct, classifiers usually deliver excellent results (assuming that the problem at hand can be solved at all).

Classification schemes can be grouped in linear and non-linear classifiers. In general, linear classifiers such as Partial Leas Squares Discriminant Analysis PLS/DA and Linear Discriminant Analysis (LDA) cannot solve non-linear problems, while non-linear classifiers will deliver solutions for both linear and non-linear cases. This does not automatically imply that one should always use non-linear classifiers, as non-linear classifiers tend to overfit

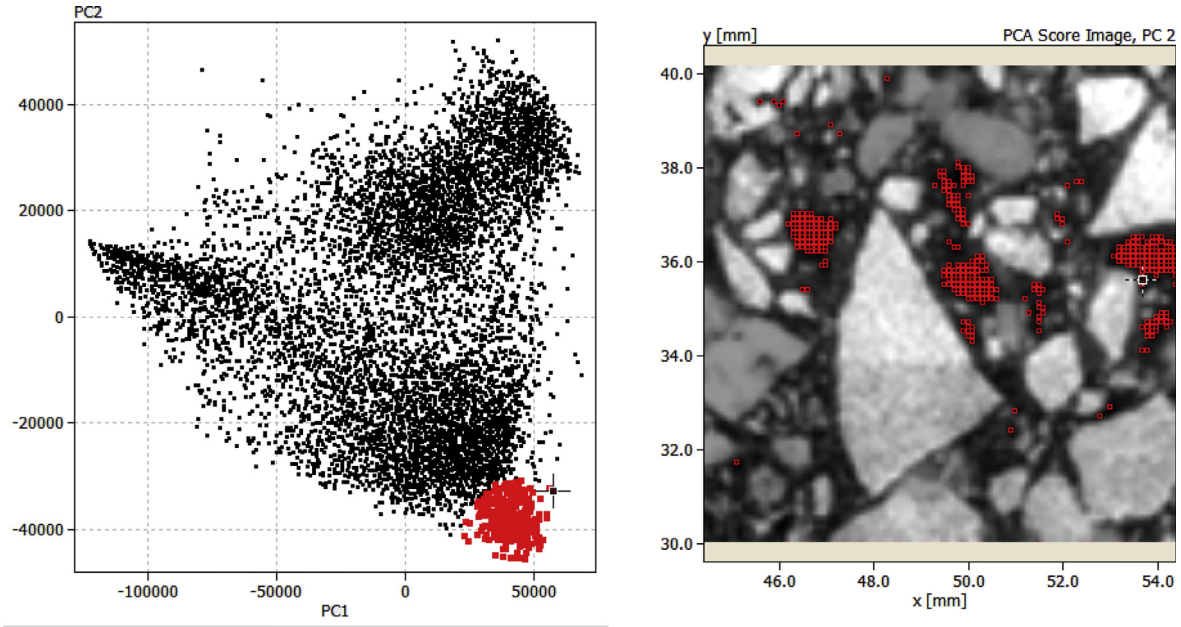

Fig. 3. Principal component analysis of the mean-centered LIBS spectra of a concrete sample. Left: score/score plot of the first two principal components. The cluster of spectra in the lower right corner has been marked. Right: the score image of the second principal component, displaying the marked pixels. The marked regions contain high concentration of calcium [dataset] [63].

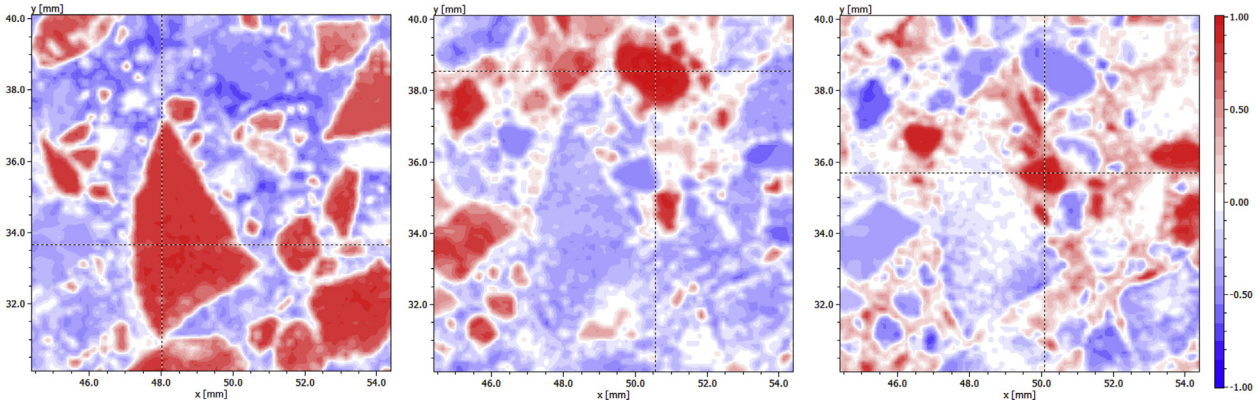

Fig. 4. Similarity maps of three different positions using the Pearson correlation of standardized spectra. Red areas indicate high spectral similarity to the location marked by the crosshair, blue areas indicate dissimilarity and white areas indicate indifferent areas (non-significant correlations). [dataset] [63].

the training data while with non-linear classifiers, this can be avoided if some requirements are met.

Most classifiers work best if configured as a binary classifier and some of the classification methods cannot be used for multi-class problems at all. In such cases it is recommended to generate binary indicator variables. Such indicator variables are derived from the class numbers by creating as many indicator variables as available classes. Each indicator variable is filled with a zero value for spectra which do not belong to the particular class and with a value of one if the spectrum belongs to this class. In this way the *k*-multiclass problem is transformed into *k* binary classification problems.

3.4.2.1. Linear Discriminant Analysis (LDA). One of the simplest linear classifiers is LDA [78]. LDA is based on a linear regression model which generates a linear surface in the p-dimensional space, effectively separating the two classes. Linear discriminant analysis suffers from the fact that multi-collinearity causes weakly determined coefficients which can result in unstable class assignments. Further, in LDA the number of variables must be well below a third of the number of pixels, which might become a problem with small images. Thus, LDA is largely replaced by PLS/DA (see below).

3.4.2.2. Partial Least Squares discriminant analysis (PLS/DA). As mentioned above the instabilities of the regression coefficients can be avoided by using PLS/DA [79], which calculates the regression coefficients of the model by using PLS [80]. As PLS is not sensitive to multi-collinearity of the variables, it does not need more samples than the number of variables. PLS/DA is an almost perfect approach to linear classification of spectra obtained from images. However, PLS requires reducing the number of factors to an optimum amount otherwise it degenerates to LDA in the case of using all factors. The optimum number of factors is determined by cross validation.

3.4.2.3. Random forests (RF). RF is one of the newer methods introduced in the field of machine learning at the beginning of this century [81,82]. RFs have proven themselves as a very reliable and powerful tool both for classification purposes and for modelling approaches. The basic principle of RFs is the combination of many de-correlated decision trees which "vote" for the final outcome within the ensemble of trees. The voting can be performed in several ways, usually by majority voting in classification scenarios. Typically, between 50 and 150 trees are sufficient to solve most classification problems. Each of the decision trees is based on a random selection of variables thus avoiding any correlation between the trees. Random forests have successfully been used to classify LIBS images of modern art materials [83] or to discriminate various polymer samples [84].

3.4.2.4. K-nearest neighbours (kNN). Another non-linear classification method is kNN classification [85]. kNN is based on the idea that the k closest objects in the p-dimensional space determine the class of an unknown spectrum (by for example, majority voting). kNN is easy to use and to calculate, however it requires having a good and correct database of known spectra. Errors in the database automatically lead to misclassifications. Further the database should have built in some redundancy so that the data space is populated by at least 10 to 20 examples per class.

There are no exact rules of the selection of *k*, however an odd *k* in the range between 3 and 9 usually works best. For a particular classifier and a particular database *k* should be determined by means of cross validation. Theoretical considerations [64] show that the error of 1NN ($k = 1$) is less than twice the Bayes error - which makes kNN some kind of a benchmark. However, kNN suffers a lot from the curse of dimensionality [86] as the distances in a *p*-dimensional space become more and more similar with increasing p.

3.4.2.5. Support vector machine (SVM). SVM [87] is an intrinsically linear classifier which can be applied to non-linear problems by applying a transformation of the data space using for examples polynomials or Gaussian density functions [88]. It can be shown that SVMs can solve non-linear problems even without explicitly calculating the non-linear transformation (this is commonly called the "kernel trick"). The basic idea of an SVM is to find a discrimination surface of finite thickness (as opposed to PLS/DA which uses an infinitely thin separating plane) which is controlled by a few points at the border of this surface. These points are called "support vectors" because they control the location and orientation of the separating surface. An application of both SVM and kNN to classifier soft tissues is given by Li et al. [89].

3.4.2.6. Artificial neural networks (ANNs). ANNs comprise a family of diverse and partially unrelated methods whose applications span a vast range of fields from pattern recognition and associative retrieval to calibration tasks. A well-structured survey on these methods can be found, for example, in the book of Du and Swamy [90].

The main problems with the quantitative analysis of LIBS spectra are spectral overlapping, self-absorption and matrix effects resulting often in nonlinear relationships between quantities and the corresponding spectral signals. These nonlinear effects can be addressed by ANNs. While there are several applications of ANNs to the quantitative analysis of LIBS data [91] imaging related analysis based on ANNs is still in its infancy. An extensive overview on ANNs and LIBS including spectral imaging is given by Koujelev and Lui [92].

3.4.3. Calibration

Calibration based on LIBS data can become quite complex if the matrix shows extreme variability, as for example in geological or biological samples. In principle, the quantification of a particular chemical element is possible by setting up a univariate regression given that the matrix is well defined, and the used spectral lines do not interfere with other elements. However, this assumption proves to be not met in many practical cases. Thus, a multivariate approach is needed to account for matrix effects and interferences.

The classical approach would be Multiple Linear Regression (MLR). However, MLR suffers from multi-collinearity of the independent variables and requires the number of training samples to be at least three times higher than the number of used wavelengths. Although there are various variable selection techniques to keep this ratio within an acceptable range, a much better approach is to use Partial Least Squares (PLS) regression. Other possibilities are random forests, artificial neural networks and the Franzini-Leoni method [93].

3.4.3.1. Partial Least Squares (PLS). PLS is certainly the most common and most mature method [80] and the setup of a calibration model is straightforward: *i)* define the independent variables (i.e. use all available wavelengths), *ii)* define the target variable to be calibrated, *iii)* find the optimum number of factors by cross validation, and finally *iv)* store and apply the found model. A good comparison of univariate regression and PLS is given by Ref. [94].

3.4.3.2. Random forests (RF). Random Forests can be used in the same way as in classification scenarios. The only difference is the voting of the individual trees of the random forest. For regression (= calibration) purposes the outputs of the individual trees should be averaged (instead of majority voting). Random forests however have one problem: they cannot extrapolate. Thus, when using random forests, it is mandatory that the training data completely cover the calibration range in order to avoid any extrapolation. More details on random forests can be found in Ref. [95].

There are several papers using random forests for calibration purposes. Wang et al. used a combination of wavelet transform with random forests where wavelets were used for de-noising the data. The de-noised and optimized variables were then fed into a random forest-based model to determine metal concentrations in an oily sludge [96].

3.5. Image fusion

Image fusion is a technique which allows to combine two images of different spectral and spatial resolution into a single image. Normally an image with high spatial but low spectral resolution (typically a monochromatic or a colour photo of the sample) is combined with an image of high spectral but low spatial resolution (i.e. the LIBS-based image). This combination results in a crisp image of the sample which is coloured according to the elemental information obtained from the LIBS measurement.

More than 10 methods of image fusion have been published, from simple arithmetic multiplication of the two images, to spectral substitution-based techniques such as the Brovey transform [97], to sophisticated calculations based on principal components or wavelets [98]. For most purposes Brovey transform delivers a very good compromise, as it is fast and delivers nice images which retain the texture of the high-resolution photo while being coloured to indicate elemental constituents.

4. Applications

In the following chapter, selected LIBS imaging applications are

presented which highlight the benefits of this analytical technique. In particular, the possibility to detect all elements of the periodic table is represented with 52 different chemical elements being analyzed in the presented works. Moreover, capabilities for simultaneous multi-element analysis is demonstrated in numerous publications. In more than 10% of the discussed applications elemental distributions of 10 or more elements were measured. Additionally, elements which are not accessible or do not allow detection with a high sensitivity with other imaging techniques are often analyzed in LIBS applications. The most common detected elements in the presented compilation of applications include mainly light elements, alkali and earth alkali elements, and non-metals. Another main benefit of LIBS is the high speed of analysis, thus large sample areas (up to several cm^2) can be analyzed in a reasonable time. Table 2 gives an overview and summarizes LIBS imaging applications allowing to conclude on the advantages this techniques has to offer. A detailed discussion of the individual publications is provided in the following chapter.

4.1. Life science

The capability of LIBS to obtain spatially resolved multi-elemental images has received increased attention. Life science applications appear to be one of the most promising field for further development of LIBS-based imaging. In this review we summarize the current state-of-the-art together with the most recent and crucial research works related to elemental bio-imaging in individual life science applications. Mainly, we tend to emphasize technical aspects of the analysis including benefits of LIBS over other analytical techniques, evidence on laser-tissue interaction, etc.

Continuous improvements in LIBS lead to further establishment of the technology among its analytical counterparts; namely LA-ICP-MS which is still considered to be the reference to LIBS. LA-ICP-MS held its position for decades in bioimaging due to its higher sensitivity and spatial resolution [99–101]. Recently, LIBS has been narrowing the gap in terms of repetition rate, cost of analysis and instrumentation affordability when insufficient sensitivity seems to be an issue of the past. LIBS fully matured in plant bioimaging [44] and becomes a viable alternative in biomedical applications [45].

The contemporary LIBS literature reflects a wide range of bio-applications where various samples (soft/hard tissues, liquids, pathogens, etc.) are analyzed under various conditions. Several LIBS reviews dealing with the analysis of biological samples or, more exactly, with their bioimaging were already published, e.g. plant material analysis [102,103], plant bioimaging [44], agriculture and food analysis [104,105], preclinical applications and medical applications [13,45,106], and veterinary and livestock applications [106].

Here we focus solely on “solid” samples and thus skip any discussion over the analysis of algae [107], pathogens with emphasis on bacteria [108], or liquid samples of biological origin [106]. The analysis of homogenized pellets is not considered, despite this approach enables easier calibration and quantitative analysis [109]. But the process of pelletization loses any information on the original tissue composition and analyte distribution. Therefore, those biological materials and/or approaches for their analysis are out of scope of this review.

Numerous ways of sample pre-treatment leading to significantly different outcomes and limitations have been presented. It is noteworthy that the sample preparation process is crucial for successful analysis using LIBS [110] and must be optimized a priori. Unfortunately, there is no established protocol of biological tissue sample preparation for LIBS analysis. The plant tissues are either fixed on top of the epoxy or pressed onto a sticky tape; potentially, cryo-fixing via flash freezing was also introduced [44,111]. Hard tissues (e.g. bones and teeth) are non-demanding. Fixing them in epoxy seems to be an appropriate approach and their cutting and polishing is then straightforward.

Fixing soft tissues is a critical step in the analytical routine [112]. Most often the researchers choose between cryo-sections and formalin fixation and paraffin embedding (FFPE). The FFPE is a golden standard in clinical applications and pathological examination of a tissue when haematoxylin and eosin staining is concerned. Thus, adapting the LIBS methodology to fit this sample preparation seems adequate. The sample may then be measured in thin sections with thicknesses approximately 10 μm. Direct LIBS analysis of paraffin blocks is also possible when providing more material for ablation and, in turn, better sensitivity. However, evidence was found indicating that the FFPE preparation of a tissue leads to unwanted redistribution of the elemental content [112]. This raises further considerations when using FFPE in metallomics applications. It is advised to use other approaches too as references to check the correctness of the sample preparation.

The parameters involved in sample preparation and consecutive laser-matter interaction make the tissue ablation a complex phenomenon. Involved parameters have convoluted dependence on laser-ablation performance and the optimization process is, therefore, tedious, and lengthy. Successful implementations of LA-ICP-MS to individual applications (e.g. plants [101] and biomedical [99]) may serve as an inspiration for LIBS research and development efforts. Both techniques have already been utilized in tandem when complementing their benefits and increasing the range of detected elements [113]. Yet still, a potential of their joint utilization is mitigated by certain discrepancies in optimal settings of laser ablation parameters.

The quantitative analysis applied directly to bioimaging of heterogeneous samples attracts considerable attention. However, any success is limited due to the essence of laser ablation itself; the need for matrix-matched standards with similar physical and chemical properties is a persistent challenge. A comprehensive review summarizing individual efforts in quantification of LIBS and LA-ICP-MS images was recently delivered [109]. As in the case of sample preparation, works on LA-ICP-MS might be an interesting source of information for further development of LIBS methodology. Several approaches have been introduced to calibrate the LIBS system. Quantification analysis of plant tissues is centered around homogenization and pelletization [111]. In the case of soft tissues, the methodology is not straightforward and contains homogenization of the tissue, utilization of inkjets or agarose gels. The most promising method so far seems to be the use of epoxy mixtures [114]. Considering hard tissues, the calibration strategies are based on calcium-rich materials, including hydroxyapatite [115] or calcium oxalate [116]. Despite all the efforts, there is still a dire need to deliver a methodology enabling accurate quantification in direct imaging of bio-samples [109]. Finally, the use of calibration-free or C-Sigma methods [117] seems promising, yet still, their implementation to bioimaging is only foreseen.

In the following paragraphs, we overview papers dealing with the imaging of plant, soft, and hard tissues. The literature research of LIBS applications is extended with the discussion over utilized LIBS instrumentation and its performance. Unifying benefits of LIBS technique which make it especially attractive over LA-ICP-MS for the presented applications are typically faster throughput and, thus, larger imaged areas; measurement of inaccessible (e.g. O, N, H) or challenging (e.g. C, P, S) elements; simultaneous detection of all analytes with no need for preselection; etc.

Table 2
Overview of LIBS imaging applications.

Sample Material	Investigated Elements	Data Evaluation	Analyzed Area (mm^2)	Reference number
Minerals	U	Multivariate	225	[37]
Minerals	Al, C, Cd, Co, Cr, Fe, H, Mn, O, P, Sn, Ti	Multivariate	468	[52]
Cultural heritage samples	C, H, Na, O	Multivariate	128	[83]
Polymers	H, K, Na, O	Multivariate	190	[84]
Soft tissue	Fe, Gd, Na, Si	Univariate	–	[113]
Soft tissue	Ca, Co, Mn, Ni, Sr, V	Univariate	–	[114]
Hard tissue	C, Ca, Cl, Fe, H, K, Mg, Mn, Na, O, P, S, Sr, Zn	Univariate	4	[115]
Hard tissue	Cd, Te, Si	Univariate	900	[116]
Plant tissue	Al, Ba, C, Ca, Cu, Fe, H	Univariate	–	[118]
Plant tissue	Cd	Multivariate	–	[119]
Plant tissue	Li	Univariate	–	[120]
Plant tissue	Cd	Univariate	–	[121]
Plant tissue	K, Mn	Univariate	1.7	[122]
Plant tissue	Er, Y, Yb	Univariate	–	[123]
Plant tissue	Cr	Univariate	–	[124]
Plant tissue	Ca, Gd	Univariate	–	[125]
Soft tissue	Ca, Cu, Gd, Na	Univariate	2	[127]
Soft tissue	Ca, Fe, Gd, Si	Univariate	–	[128]
Soft tissue	Ca, Na	Univariate	–	[129]
Soft tissue	Fe, Mg, Si	Univariate	–	[131]
Soft tissue	Al, Cu, Fe Mg, Na, Si	Univariate	–	[133]
Soft tissue	Ba, Ca, Fe, Na, Sr	Univariate	–	[134]
Hard tissue	Al, Ca, Na, P	Univariate	–	[137]
Hard tissue	Fe, Si	Univariate	–	[138]
Soft tissue	Cd	Univariate	–	[139]
Immunoassay	Ag	Univariate	–	[143]
Immunoassay	Au, Eu, Nd, Pr, Yb	Univariate	–	[144]
Immunoassay	Ag, Al, Ca, Cu, Fe, Mg, Si, Zn	Univariate	–	[145]
Mine core	Al, Fe, Mg, Mn, Na, Si, Sr	Univariate	1600, 750	[146]
Speleothem	Al, Ca, Fe, K, Mg, Na, Si, Sr	Univariate	2000	[147]
Speleothem	Ca, Mg	Univariate	72	[148]
Shells	Cu, Mg, Pb, Si, Zn	Univariate	–	[149]
Minerals	Ce, Cu, Fe, La, Si, Y	Univariate	470	[150]
Minerals	Al, As, B, C, Ca, Cu, Fe, Mo, P, S, Si, Ti, Zn	Univariate	–	[151]
Mine core	F, O	Univariate	15, 200	[152]
Minerals	Al, Ca, Si	Univariate	16	[153]
Minerals	Al, Cu, Fe, Mg, P, Si	Univariate	0.6	[154]
Carbonaceous shale	Al, Ca, Fe, K, Mg, Na, Si	Multivariate	29	[155]
shale	Al, C, Ca, Fe, H, Mg, O, Si	Univariate	64	[156]
Ore	Al, Ca, Cr, Cu, F, Fe, K, Mg, Mn, Na, Ni, P, S, Si, Ti, Zr, Pd, Pt	Multivariate	10000	[157]
Minerals	Al, Ca, Cu, Fe, K, Mg, Na, Ni, Pd, Pt, S, Si	Univariate	1200	[158]
Cultural heritage samples	Al, Cu, Fe	Univariate	–	[163]
Cultural heritage samples	Al, Ca, Fe, K, Mg, Na, Si	Univariate	–	[164]
Cultural heritage samples	Ca, Mg, Si	Univariate	–	[165]
Cave walls	Mg, Si, Sr	Univariate	–	[166]
Cultural heritage samples	Al, C, Ca, Cu, Na, O, S, Si	Univariate	0.8	[167]
Limestone	C, Ca, Fe	Univariate	625	[168]
Steel	Al, Mn, N, O	Univariate	100	[171]
PCB	Al, Au, Ba, Ca, Co, Cu, Fe, K, Li, Mg, Mn, Na, Ni, Sb, Si, Sn, Ti, Zn, Pb	Multivariate	1200	[172]
Thin films	Ba, Cu, Mg, Mn, Y	Univariate	–	[173]
Composite material	C, Co, Cr, Fe, Ni, Si, W	Univariate	0.81	[174]
Catalyst	Pd, Pt, Rh	Univariate	345	[175]
Catalyst	Al, CN, Fe, Pd	Univariate	–	[176]
Catalyst	Al, C, Ni, S, V	Univariate	–	[177]
LLZO	Al, La, Li, Zr	Univariate	1.23	[178]
LLZO	La, Li, Fe, Zr	Univariate	–	[179]
$LiCoO_2$	Co, Li	Univariate	0.25	[180]
Concrete	Ca, Cl, Na	Univariate	0.04	[181]
Lithiated tungsten	Ar, Ca, H, K, Li, Na, O, W	Univariate	26.4	[182]
Lithiated tungsten	Li, Si, Ti	Univariate	–	[183]
Nuclear waste	Al, Ca, Eu, Fe, La, Mo, Nd, Pr, Sr, Zr	Univariate	1.9	[184]
Gunshot residues	Ba, Pb, Sb	Univariate	21450	[185]
Tablets	Fe, Ti	Univariate	4	[186]
Tablets	K, Mg, Na	Univariate	4	[187]
Solar cell material	Cu, Ga, In, Se	Univariate	6.6	[188]
Piezoelectric crystal	Ca, Zr	Univariate	225	[189]

4.1.1. Imaging of plant tissues

In the last two decades LIBS became an established analytical tool in the plant bioimaging. This issue has already been addressed in several studies and review publications [44,102,104,111]. It is noteworthy that we avoid any discussion of food analysis [104,105].

LIBS technique excels over other analytical techniques mainly in terms of affordable instrumentation enabling large-scale mapping. Such instrumentation provides reasonable analytical performance (sensitivity) and is, thus, a vital alternative in many applications. The imaging of macro- and micro-nutrients is a great added value

of LIBS when high number of whole plants (or their parts – roots, stems, leaves) are scanned. The control of nutrient contents is of paramount interest while plants suffer from various stress during growth, e.g. draught, insufficient sunlight, under- or over-fertilization, toxic environment. The latter then extends the number of applications into environmental monitoring and the uptake, accumulation and translocation of toxic and heavy metals.

The most recent bioimaging plant review [44] deals in great details with the novelty of using LIBS as a new instrumental method in the spatially resolved single/multi-element analysis of various plant samples. The paper comprehensively describes the analysis of various plant species, plant tissues as well as detection of different analytes as essential elements (K, Ca, Mg, P, Fe, Mn, Cu, and B), non-essential elements (Pb, Cd, Ag, Si, Li, Y, Yb, and Cr), several types of nanoparticles (silver, cadmium telluride, and photon-upconversion nanoparticles) or even pesticide (chlorpyrifos).

A recent work [118] studies the translocation of two types of cadmium telluride NPs (CdTe quantum dots and CdTe quantum dots cover by silica shell) together with free Cd (II) ions by using two different LIBS approaches. Selected plants (white mustard) were exposed to test compounds for 3 days, then the plants were washed, dried, epoxide glued onto glass slides, and then LIBS analysis was performed. Firstly, the whole plants were measured in a raster of spots with a 100 μm step (giving the lateral resolution). Then, only the important or somehow interesting plants parts where measured with the step 25 μm, in so-called micro-LIBS setting, to show exact place of cadmium bioaccumulation sites and to demonstrate different behaviour of cadmium in plants based on his source (see Fig. 5).

A recently published approach in LIBS plant analysis shows a spatially resolved root-rhizosphere-soil image in wider context of plant in its natural environment [119]. LIBS elemental images visualize the nutrient exchange in plant rhizospheres and organic/inorganic content in switchgrass. The live root sampling was demonstrated in plant analysis and the drill press for sectioning frozen stabilized soil. Multi-elemental images of roots (and rhizospheres) in surrounding soil for H, C, O, P, K, Ca, Mg, Fe, Si, Al, Mn, and Zn were shown with 100–150 μm lateral resolution. Based on plotted maps and principal component data analysis the elements profiles in soil depending on their distance from roots could be assessed. This approach offers detailed information at the scale, which has clear implications for various soil/plant science challenges (e.g. phytoremediation or effects of fertilizers on agricultural yields).

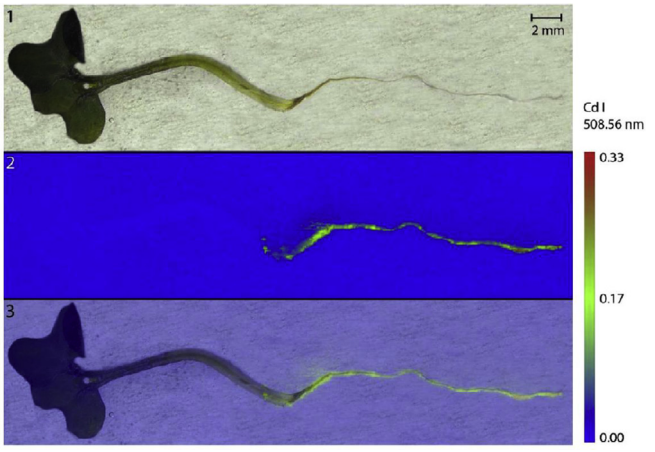

Fig. 5. Example of LIBS elemental images obtained for plants. 1. Photograph of Sinapis alba plant exposed to CdTe QDs at the nominal concentration 200 mM Cd before LIBS measurements. 2. LIBS maps constructed for Cd I 508.56 nm (spatial resolution of 100 μm). 3. Overlap of the original photograph of the plant with LIBS map. The scale shows the total emissivity of the selected emission lines [118]. Reprinted from "Detail investigation of toxicity, bioaccumulation, and translocation of Cd-based quantum dots and Cd salt in white mustard", 251, Pavlína Modlitbová, Pavel Pořízka,Sára Stříteżská,Štěpán Zezulka, Marie Kummerová, Karel Novotný, Jozef Kaiser, 126174, 2020), with permission from Elsevier.

The current state of the LIBS plant bioimaging can be summarized by the following highlights. In the last two decades LIBS plant analysis made a great step forward due to not only an improvement in LIBS instrumentation (sensitivity, speed, and spatial resolution of analysis) and in plant sample preparation, but mainly by using obtained LIBS maps in interdisciplinary research works [119], by involving of plant toxicity testing [120], and by searching for interesting and novel applications in imaging of Li in the plant leaves [121] and nanoparticle enhanced detection [122]. Recent work presents the possibility of in situ plant analysis in field conditions [123], 3D-model compilation of element distribution in leaves [123], and nanoparticles localization [124].

The best achieved spatial resolution in plant analysis has been recently improved to 25 μm [119], this value is already close to commonly used LA-ICP-MS spot sizes, where the lateral resolution is in the range of 1–500 μm [101]. Zhao et al. [122] demonstrated a novel idea of deposition Ag nanoparticle on the plant surface in order to achieve a sensitivity enhancement (limit of detection (LOD) for phosphorus were found to be improved by two orders of magnitude) in Nanoparticle Enhanced LIBS (NELIBS) experiments. Double pulse LIBS arrangement was employed as another way of signal enhancement [125]. Furthermore, the information on the spatial distribution of selected elements can be used as a valuable information showing the relationship between the exact location of an element and its effect. This effect could be negative (even toxic) - [122] as well as positive [126] for plant development, it depends on the chemical species of the element and its concentration, and also the type of monitored plant as the effects are specific to each organism.

4.1.2. Imaging of mammal tissues

4.1.2.1. Soft tissues. The LIBS technique repeatedly proved its bioimaging applicability for tracing uptake, transport, distribution, and bioaccumulation of macro- and micronutrients, nanoparticles, and non-essential elements in several organisms (mouse, human), organs (kidney, lung, skin), and diseased tissues (skin or lung tumours) as was summarized in three most recent reviews [13,45,106].

Elemental variations can be effectively used as an indicator of malignancy and to monitor its stage and progression. Therefore, the analysis of metallomes (metalloproteins, metalloenzymes and other metal containing biomolecules) undergoes intense research. The main research target of metallomics is the elucidation of metallomes' biological or physiological functions during physiological and pathological alterations of tissues. Incorporation of spectroscopic methods can fill knowledge gaps in these biological processes. Any changes in the elemental composition induce significant alteration of further tissues' growth, pathological processes, and even initiation and progression of a carcinoma.

The body of work published by the Vincent Motto-Ros' group bring tremendous progress in terms of spatial resolution and scale of the analysis; the distribution of elements in mouse kidneys [114,127–131], mouse tumours [132,133], and healthy human skin or human skin melanoma [134] was imaged. Outside of their works, the human malignant pleural mesothelioma (lung tumour) was investigated using LIBS multi-element mapping [113]. All these studies showed LIBS as an advanced analytical platform providing large-scale elemental imaging of heterogeneous sample surfaces. Also, the great accessibility for assessment of nanoparticles was

demonstrated by detection of gadolinium-based nanoparticles in mouse kidneys [130].

It is noteworthy that the sample preparation process is crucial for successful bioimaging in LIBS and has be to be optimized a priori for each experiment as summarized in review by Jantzi et al. [110]. There is no established way of soft tissue sample preparation for LIBS yet. Vincent Motto-Ross' group early stage research papers recommend the use of sample cryo-sections [128,129]. However, in their latter work improved detection was obtained by using epoxy fixing of samples after dehydration in a series of ethanol solutions [114,130], see Fig. 6. On contrary, Bonta et al. [113] compared the cryo-cutting and paraffin embedding after formalin fixation (the gold standard in histological tissue preparation) and found that paraffin fixation influences the distribution of certain elements. Moreover, the soft tissue sections were planted on silicon wafers instead of glass slides (as it is the most common), which led to improvement in sensitivity.

The thickness of the cross-section is of interest in order to supply sufficient amount of material for laser ablation and to reach satisfactory sensitivity. An effort is being invested in fitting laser spectroscopy to standard histological routines (to complement e.g. haematoxylin and eosin staining with minimum extra sample handling). However, the histology demands thinner sections (up to 5 μm) and laser-ablation demands more material in the interaction spot and thus thicker sections are preferable (from 10 μm).

Finally, the phenomenon of and parameters affecting the laser-tissue interaction are being extensively investigated. Detailed description of pulsed laser ablation of soft tissues is given elsewhere [135]. LIBS instrumentation and individual parameters were comprehensively summarized by Jolivet et al. [13].

4.1.2.2. Hard tissues. The pulsed laser ablation of hard tissues is less demanding in terms of analytical LIBS performance when compared to the case of soft tissues. Therefore, there are many pioneering works that utilized LIBS in the imaging of hard tissues (e.g. bone, teeth) where imaging was substituted with less demanding line scans. Former LIBS review publications have also mentioned the imaging of hard tissues (also referred as biominerals or calcified tissues) [102,106]. Another publication [136] brings a detailed review on the utilization of LIBS in the analysis of biominerals going well beyond the imaging point of view.

From the biological point of view, the imaging of biominerals targets wide selection of elements [136]. First, the major interest is in the detection of Ca and P forming the mineral phase and to macro elements such as C, O, N, and H relating the signal to organic phases (e.g. proteins). Detection of essential elements (Cu, Mn, I, Sr, Zn, etc.) indicates changes in the function of organs and nutrition. Finally, the uptake and accumulation of trace metals (Pb, Hg, Cd, As) shows potential malnutrition or long-term exposition to toxic environment.

The analysis of hard tissues may be divided into two main directions: *i)* monitoring of uptake and accumulation of various elements in tissues and *ii)* detection of qualitative difference between healthy and diseased tissue. The former case leads to nutrition habits or malnutrition when the cross-section of a tooth is imaged, e.g. the ratio of Sr/Ca was used to characterize a bear tooth [137]. The latter case, the imaging discovers correlations between the diseased tissue and increase/decrease in content of major or minor elements [138].

4.1.2.3. Tag-LIBS. Recently, traditional optical and spectroscopic methods evaluating the immunoassay results (absorbance, fluorescence, and luminescence) are being complemented with laser-ablation based spectroscopy methods [44]. Spectroscopic techniques are adapted to standard routines and benefit the researcher with an alternative insight. Apart from the simple label readout, accurate qualitative and quantitative chemical (i.e., elemental or molecular) information is obtained.

The utilization of NPs across various applications has also influenced the LIBS community. NPs are vitally used for signal enhancement in the laser ablation of selected analytes. LIBS was already used as a readout method for NP-based labels in the so-

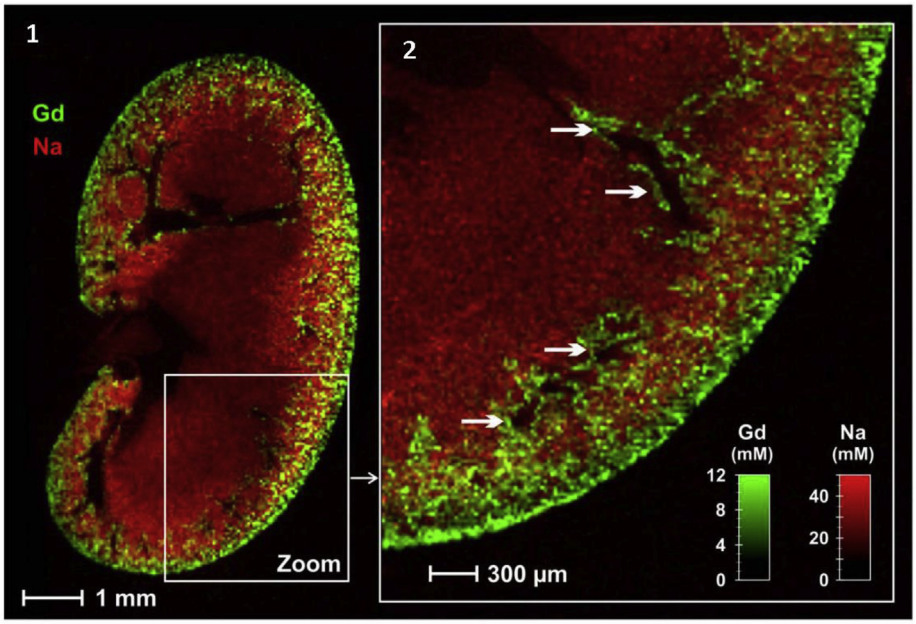

Fig. 6. Example of LIBS elemental images obtained for soft tissues. 1) Gadolinium (green) and sodium (red) distributions in a coronal murine kidney section, 24 h after gadolinium nanoparticle administration (spatial resolution of 40 μm). 2) Magnification of the image presented in (1.) in an adjacent section with 20 μm resolution. The white arrows indicate regions that are lacking in tissue, corresponding to blood vessels and collecting ducts [114]. Reprinted by permission from Springer Nature: Springer Nature, Scientific Reports, Laser spectrometry for multi-elemental imaging of biological tissues, L. Sancey et al., 2020.

called Tag-LIBS; which was introduced almost a decade ago [139]. Ovarian cancer biomarker CA-125 conjugated with silica microparticles reached ppb-level limits of detection. From this success, several patents stemmed [140,141].

The concept of Tag-LIBS is straightforward: the proteins (biomarkers) within the tissue are selectively bonded to metallic nanoparticles. The sample is then scanned, and the LIBS signal of NPs is imaged. Then, the distribution of targeted proteins (e.g. cancer) is imaged indirectly through the presence of NP-signal. The biggest advantage is that the NPs may be engineered in various way in order to be strictly specific to selected protein [142]. Such concept has a great potential in large-scale analysis of cancerous tissues when it could circumvent the relatively poor limits of detection of LIBS technique. However, intense research and sample pre-treatment optimization is needed prior the full exploitation of the Tag-LIBS.

LIBS was further developed as a vital readout technique for various pathogens and proteins. Metallothionein was deposited on a polystyrene microtiter plate and detected via its conjugation with Cd-containing quantum dots [143]. Au and Ag NP labels were examined from the bottom of a standard 96-well microtiter plate; a sandwich immunoassay for human serum albumin using streptavidin-coated Ag NP labels was developed [144]. Most recently, LIBS was implemented for the analysis of lateral-flow immunoassays with Au NPs labelled *Escherichia coli* [145]. Fluorescence and atomic absorption spectrometry were typically provided as reference techniques.

4.2. Geoscientific studies

Investigation of the distribution of different elements within rocks, sediments, corals, and shell samples offers insights into past, present, and future development of the climate. As mappings of large areas, desirable with resolution in the low μm range, is often necessary, LIBS is a very promising technique for paleoclimate studies as it offers very fast mappings [146]. Cáceres et al. [147] report the possibility to perform megapixel elemental images of different large samples such as speleothems (calcium carbonate cave deposits) and corals (calcium carbonate skeletons) using LIBS. This study presents the advantages of mapping large areas with a high lateral resolution for paleoclimate studies.

Speleothems were also investigated using LIBS by Ma et al. [148] that report the distribution of relative elemental concentrations of major, minor as well as trace elements. The list of investigated elements includes Ca, Na, Mg, Al, Si, K, Fe and Sr. By evaluating compositional correlations, mineral phases within the speleothems were identified. In the work of Hausmann et al. [149], Mg and Ca concentration ratios were mapped in shell carbonate, which is a type of sample often used in paleoclimatic and environmental studies. This work mainly focused on the development of an automated, high-throughput LIBS system for the analysis of these types of samples.

Fabre et al. [150] evaluated the use of LIBS for spatially resolved mineral characterization. Different phases of the investigated minerals were analyzed within a 5 cm^2 sample area with a lateral resolution of 15 μm. This study demonstrated the advantages of LIBS when it comes to mapping of large sample areas. Additionally, they also reported the detection of some rare earth elements (La and Y) in LIBS imaging experiments using a laser spot size of 10 μm. Challenges in the data evaluation of megapixel elemental images of complex multi-phase samples were also addressed. Imaging of rare earth elements in minerals was shown to be possible by combining LIBS with plasma-induced luminescence (PIL) by Gaft et al. [151]. For the detection of elements that are relevant to mineralogy (e.g. S, P, As, B, C or Zn) and have strong emission lines in the vacuum ultraviolet (VUV) wavelength range, Trichard et al. [152] reported the use of a VUV probe during mapping in a mining ore under ambient conditions. They achieved a detection limit of 0.2 wt% for sulfur in a single-shot configuration. In the work of Quarles et al. [153], the unique ability of LIBS to detect F was used to map F in bastnäsite mineral. Additionally, quantitative results were obtained by using in-house prepared standards based on NIST SRM 120c.

3D elemental distributions of rare earth elements in the mineral Bastnäsite were reported by Chirinos et al. [154], who used a combined setup incorporating LIBS and LA-ICP-MS. They revealed that new possibilities can be achieved by this combination, such as an expanded dynamic range or the joint 2D/3D visualization of elements and isotopes. Such a setup enables the detection of each element with the more suitable technique, which was demonstrated via the example of calcium: LIBS has a high sensitivity for Ca whereas LA-ICP-MS suffers from interferences due to which usually the less abundant isotope ^{44}Ca has to be measured.

In order to boost sensitivity, a double-pulse LIBS system was employed by Klus et al. [37] for the high resolution mapping of uranium distribution in sandstone-hosted uranium ores. Different data-evaluation strategies were also investigated in this work. Moncayo et al. [52] demonstrated the applicability of PCA for dataset reduction and for the exploration of megapixel elemental maps of a turquoise sample. Shale samples were imaged in a study conducted by Xu et al. [155]. In this study, the existence of a local thermodynamic equilibrium (LTE) was assessed and confirmed on the mapped area of the sample. As electron density and excitation temperature was also confirmed on the mapped area, a linear conversion of emission line intensities to concentrations was performed. Prochazka et al. used a combination of double-pulse LIBS with high resolution X-ray computer tomography to provide volumetric information of the elemental distribution in minerals [35]. Another study on shale samples was carried out by Jain et al. [156]. In this work, shale samples taken at various depths were analyzed and mapped using LIBS. Using the unique feature of LIBS to detect C and H, it was possible to detect and map these elements. Additionally, quantitative results for these elements were obtained by characterizing some of the samples using CHN-analysis and using these as calibration standards for LIBS.

As LIBS usually allows detection of emission signals over a broad spectral range, multivariate data evaluation strategies are commonly employed, which support not only elemental mapping but also spatially resolved sample classification. Meima et al. [157] investigated the applicability of a spectral angle mapper (SAM) algorithm for the laterally resolved classification of different minerals in ore samples. Several base metal sulfides, rock-forming minerals, accessory minerals, as well as several mixed phases making up the main borderline between different mineral grains were successfully classified in the recorded images. Rifai et al. [158] used PCA for the identification of different minerals in a platinum-palladium ore. With this approach, seven different minerals were identified and correlated with the generated maps. Quantitative multiphase mineral identification was also carried out by Haddad et al. [159] using a multivariate curve resolution – alternating least square (MCR-ALS) method. Obtained results were evaluated and in good agreement to conventional EDS-SEM analysis. Therefore, LIBS proves to be a very useful tool for mineral identification in mining operations as it can be employed in an online-setup.

The EU regularly updates its list of critical raw materials (CRM) and their governance levels. These strategic documents list a number of inorganic elements and materials, which are highly demanded by current industrial technologies, but for which the supply is limited within the EU [160]. The high demand for some of these elements and materials already increased their price on the market, which in turn made mining and metallurgical processing of

their ores economical in a significantly lower concentration than before. Consequently, assessment or re-assessment of geological formations potentially containing these elements/materials is in progress everywhere in the EU. Considering that some of the elements on these CRM lists are light elements (e.g. Be, Li, B, F) that are not easy to detect by other techniques, LIBS has a great prospect in these explorations. For example, Fig. 8, shows LIBS elemental maps of a granitoid rock sample for Be, studied by Jancsek et al. [161]. The map reveals that out of the four mineral grain types studied, Be and Bi is present in the highest concentration in biotite and amphibole, which suggests that mainly these minerals should be mined. Such LIBS imaging carried out by portable, stand-off instrumentation has the potential to be able to seriously speed up the assessment of the supplies (see Fig. 7).

4.3. Cultural heritage studies

LIBS imaging experiments can provide important information about art or historical items. Elemental fingerprints can be used for provenance studies and to assess the authenticity of samples. This information can be well augmented by elemental imaging data that can shed light on the fabrication process of the artefacts. One of the first applications of LIBS imaging in the field of cultural heritage science was presented at the first LIBS Conference in the year 2000 by Corsi et al. [162] investigating the elemental distribution of a roman fresco by analysing a 11x11 grid on the sample. As LIBS also offers remote analysis, historical objects can be analyzed directly in museums without bringing the sample to the laboratory. Grönlund et al. [163,164] were the first to report remote imaging of cultural heritage objects using a fully mobile LIDAR system operating at a wavelength of 355 nm mounted on a Volvo F610 truck. In this work, the spatial arrangement of different metal plates was identified over a distance of 60 m. In a study by Fortes et al. [165], elemental images of the façade of a cathedral in Malaga were recorded using a portable LIBS system. This data allowed the evaluation of Si/Ca and Ca/Mg intensity ratios and hence the identification of construction materials.

Alterations of cave walls, which poses a challenge when it comes to preservation of cave art, were investigated by Bassel et al. [166]. In this study, mainly coralloid formations were investigated using a portable instrument for spot measurements in the cave but imaging experiments were also carried out in the laboratory. Major elements (Si, Al, Fe, Ca, Mg, Na, K) as well as minor and trace elements (Li, Rb, Sr, Ba) were detected.

While the use of portable LIBS systems allow analysis of samples that otherwise would not be possible as the sample can not be brought into a laboratory, these systems usually come with some limitations compared to more sophisticated lab-based LIBS systems. These limitations usually involve sensitivity and spectral or lateral resolution. Double-pulse or tandem LA-ICP-MS/LIBS instrumentation, which are only available in more sophisticated setups, can also be used to improve the quality of analysis.

Syta et al. [167] reported the combined use of LIBS and LA-ICP-MS imaging to investigate medieval Nubian objects with displaying specific blue paintings whether they are Egyptian blue ($CaCuSi_4O_{10}$) or lapis lazuli ($Na_{8-10}Al_6Si_6O_{24}S_{2-4}$). By elemental mappings of cross-sections of various samples and using Na and Cu as elemental markers, the identification of these two inorganic pigments was achieved. Weathering of historical limestone samples from Italian urban environments were investigated by Senesi et al. [168] using double-pulse LIBS 3D imaging. The double-pulse approach allowed for high resolution and 3D elemental mappings of a degradation layer present on the investigated weathered limestone. A decrease of Al, Fe, Si and Ti line intensities and an increase of Ca line intensity with depth in the degradation layer was found and was ascribed to decreased atmospheric pollution effects at greater depths.

Bulk classification of various materials relevant for the field of cultural heritage has already been performed in several works [169,170]. In the work of Pagnin et al. [83] the capabilities of LIBS for the spatially resolved classification of contemporary art materials consisting of inorganic pigments and organic binder materials was investigated. A multivariate classification model was established that allows the classification of mixtures of 9 different inorganic pigments and 3 different organic binders. The developed classification model was used for the laterally resolved classification of these materials within a structured sample (Fig. 9).

4.4. Materials science

Materials science uses and develops a range of materials. These materials can vary widely in their chemical composition, as they include e.g. alloys, steel, ceramics, glasses, polymers as well as composites. All these materials must comply with criteria set up for their physical and chemical properties for their successful application – whether these criteria are met or not is often tested by homogeneity and chemical composition analysis. Therefore,

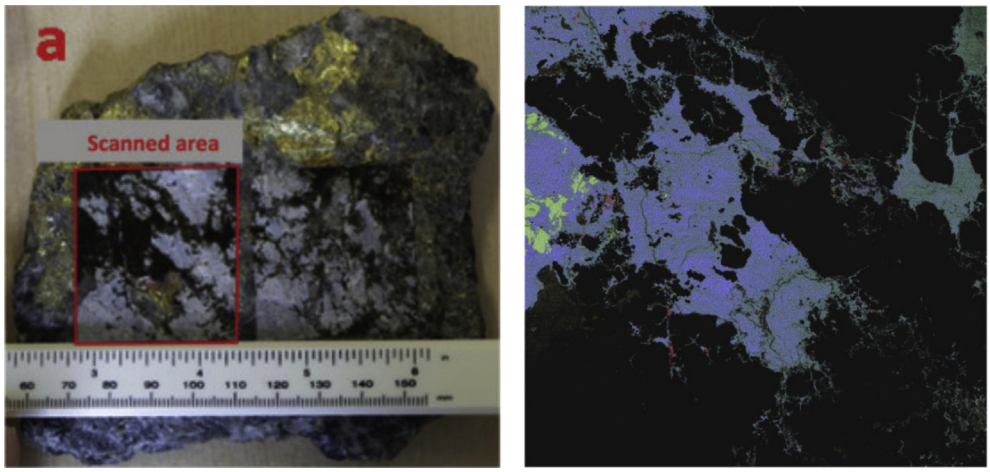

Fig. 7. Chemical mapping of an area of 40 × 40 mm^2, composed of 1602 × 1602 pixels, on the rough surface of the rock, showing the spatial distribution of Fe (green), Cu (blue), Zn (red), Ca (cyan), Ag (magenta) and Al (yellow). The dark area corresponds to the absence of LIBS signal in the crystalline mineral (silicates) under our experimental conditions. The spatial resolution (laser spot size and step size) is 50 μm [146]. Reprinted from Spectrochimica Acta Part B: Atomic Spectroscopy, Volume 150, K. Rifai et al., LIBS core imaging at kHz speed: Paving the way for real-time geochemical applications, 2018, with permission from Elsevier.

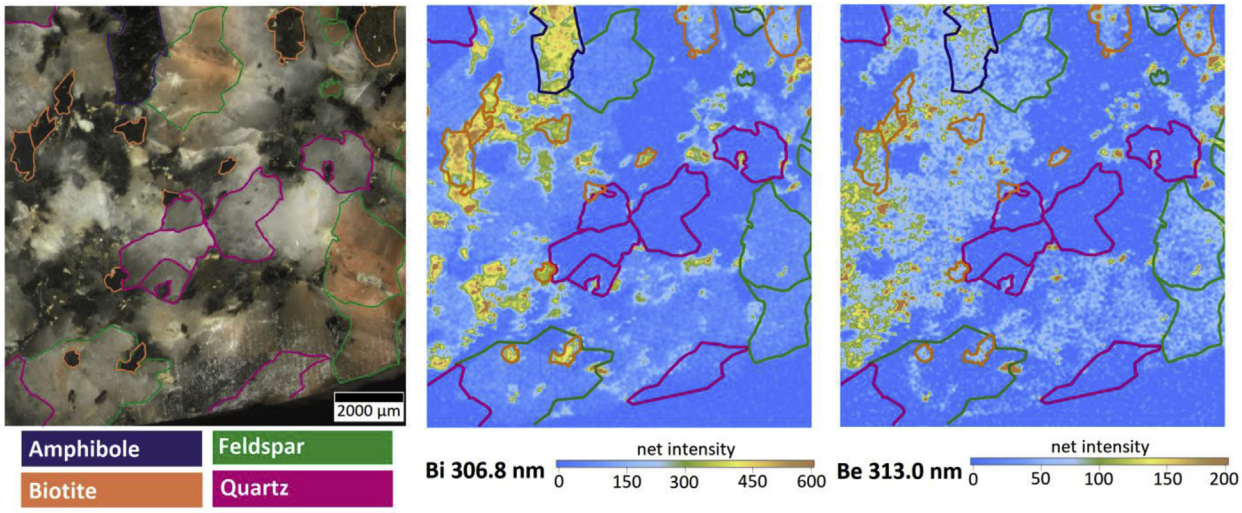

Fig. 8. Light microscope (on the left) and LIBS chemical imaging (on the right) of a granitoid sample taken from Mórágy, Hungary. Location of the four mineral grain types (quartz, feldspar, biotite, and amphibole) in the rock are indicated by coloured contour lines [161].

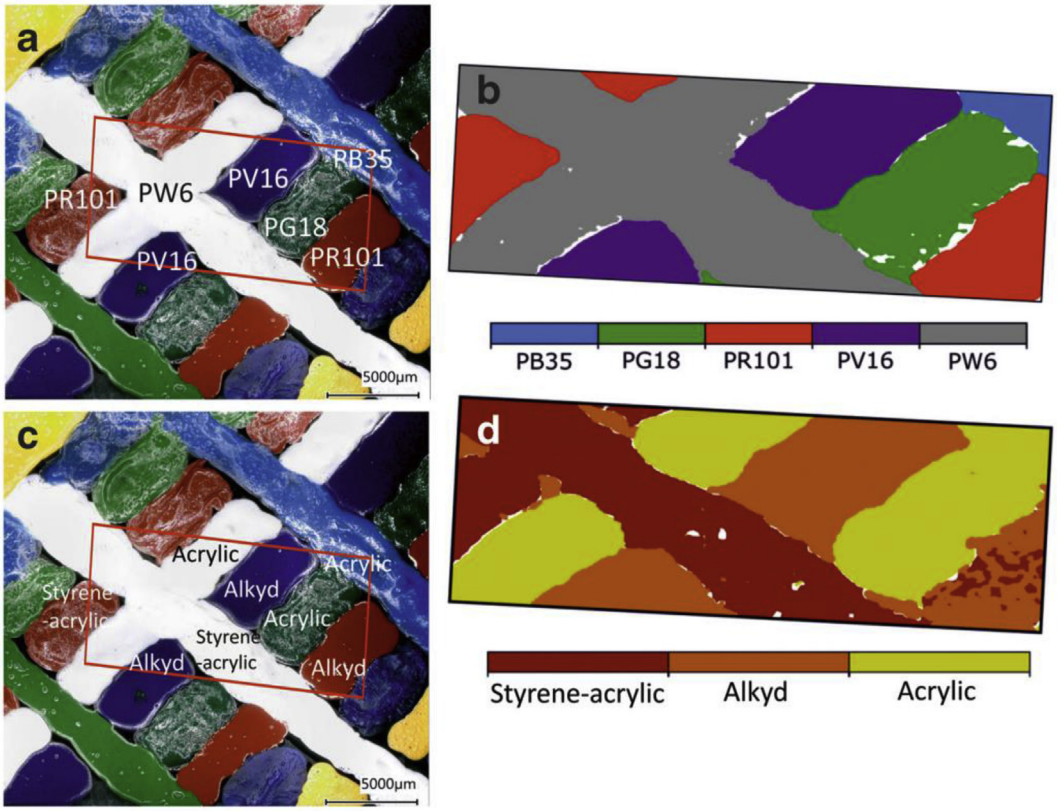

Fig. 9. Laterally resolved classification of contemporary art materials using LIBS. a) microscope image with marked distribution of different inorganic pigments, b) predicted distribution by a random decision forest of the distribution of inorganic pigments, c) microscope image with marked distribution of organic binder materials and d) predicted distribution by a random decision forest of the distribution of organic binder materials [83]. Reprinted by permission from Springer Nature: Springer Nature, Analytical and Bioanalytical Chemistry, "Multivariate analysis and laser-induced breakdown spectroscopy (LIBS): a new approach for the spatially resolved classification of modern art materials", L. Pagnin et al., 2020.

elemental imaging techniques such as LIBS are very useful to investigate novel materials, derived information is often very useful for further improvement of material properties as well as for the monitoring of production/synthesis procedures.

Alloys, or eminently steel, are amongst the most widely applied materials and are therefore of great interest for research. In the work of Bette et al. [171] LIBS elemental imaging was performed for the first time with repetition rates of 1000 Hz. In this work, steel samples were analyzed with a special focus on detecting non-metallic inclusions such as sulfur and phosphorus.

Recycling of electronical waste is becoming more and more important. Mappings of printed circuit boards were carried out by

Carvalho et al. [172]. LIBS data combined with multivariate data evaluation strategies (PCA) was used to investigate metal distributions within the boards. The authors were able to identify and map 18 elements within the sample. The described results are valuable for the research of new recycling strategies for electronic waste.

Bulk materials are often covered with thin films to enhance their physical and/or chemical properties. Thin films of copper, as well as $YBa_2Cu_3O_7$ (YBCO) - a high-temperature superconducting material - were investigated in the study of Ahamer et al. [173]. A fs-LIBS system was employed to perform high resolution elemental and molecular imaging of the thin film. Composite wear-resistance coatings made of 1560 nickel alloy reinforced with tungsten carbide was analyzed by Lednev et al. [174]. In this work, LIBS was used for 3D imaging experiments with a special focus on the analysis of C and Si which were not detectable with SEM/EDX. Besides C and Si, also Fe, Ni, Cr, W and Co were detected with LIBS.

Heterogeneous catalysis is a field important for various applications in the chemical industry or e.g. in the exhaust systems of cars. Mesoporous alumina is often used as a support. Investigation of the lateral distribution of the active material across the surface of the catalyst, but also of contaminations in the mesoporous alumina in spent catalysts offers an important insight into catalytic processes. Compared to EPMA, which is conventionally used for elemental mappings in the field of catalysis, LIBS enables analysis of light elements. LIBS imaging experiments were already conducted in 1999 in this field by Lucena et al. [175], who investigated the distribution of platinum group metals (PGMs) in car catalysts. Trichard et al. [176] use LIBS for the quantitative imaging of Pd in catalysts. In their follow-up work [177] Trichard et al. reported successful quantitative imaging in heterogeneous catalyst samples impregnated up to 53 days with asphaltenes. LIBS was not only able to detect S, C and Al, but also Ni and V, which are only present in the trace (ppm) range. By transforming the 2D maps to 1D profiles, transport mechanisms of the investigated materials within the alumina substrate were assessed.

With the strongly going industrial application of Li-ion batteries, a lot of research focuses on developing novel materials which could improve the performance of these batteries. Hou et al. [178] investigated LLZO ($Li_7La_3Zr_2O_{12}$), a promising novel material for a solid-state electrolyte, by using fs-LIBS to perform 3D elemental analysis with a special focus on elemental ratios of Li/La, Zr/La and Al/La. The reported depth resolution was an impressive 700 nm. Interface formation between a Li electrode with an LLZO electrolyte were investigated by Rettenwander et al. [179] using LIBS imaging combined with other analytical techniques. LIBS images revealed the formation of a Li deficient interlayer at the interface. Li-ion cathode material $LiCoO_2$ was analyzed by Imashuku et al. [180]. Li/Co ratios were quantified and investigated in cycled cathode materials. Even though the precision of obtained quantitative results is not comparable to conventional X-Ray Absorption Spectroscopy (XAS), LIBS results can still be used to obtain semi-quantitative results.

Concrete is one of the most important construction materials for roads, bridges, tunnels, buildings, etc. hence the monitoring of the degradation and changes of its properties is crucial. For example, the distribution of various species harmful to concrete, such as Cl^-, Na^+, SO_4^{2-}, is of great interest as it can promote the assessment of the expected lifetime of the structures. As these species are only harmful if they are present in specific phases within concrete, the differentiation between the cement phase and agglomerates is also necessary. Gottlieb et al. [181] reported the use of LIBS in combination with an expectation-maximization (EM) algorithm for the cluster analysis of different phases present in concrete. This approach made it possible to exclude non-relevant aggregates from the analysis area.

The uses of polymers ranges from packaging over composite to construction materials. In some applications, polymers are used as a bulk material, however, materials consisting of multiple polymer layers are also often used in e.g. food packaging. A study demonstrating the capabilities of LIBS to map the distribution of different polymers within a sample was carried out by Brunnbauer et al. [84]. 2D mappings as well as 3D depth-profiling of structured polymer samples were carried out and the distribution of the different polymer types present in the sample were classified using multivariate statistical methods.

Due to its ability to perform remote analysis, LIBS inherently has advantages over other techniques when analysing dangerous or hazardous materials, for example in nuclear applications. Li et al. [182] and Hai et al. [183] carried out studies regarding the Experimental Advanced Superconducting Tokamak (EAST) fusion reactor located in Hefei, China. In the first study by Li et al., 2D analysis as well as depth profiling of Li on a W wall employed in the EAST fusion reactor as a plasma facing material (PFM). Hai et al., recorded distribution of impurities (H, O, Ar, K, Na, and Ca) on lithiated tungsten employed in reactor walls. Investigations regarding nuclear waste using LIBS were carried out by Wang et al. [184] with a special focus on the long-term migration of Mo, Ca, Sr, Al, Fe and Zr and various rare-earth elements.

Lately, LIBS imaging has also found its way into forensic science, where López-López et al. [185] et al. successfully employed LIBS mapping experiments for the visualization of gunshot residues. In this work, elemental markers such as Pb, Sb and Ba were used to investigate the distribution of residues as a function of their distance from clothing targets.

Pharmaceutical tablet coatings were investigated using 3D depth profiling by Zou et al. [186]. In this work, coating thickness, coating uniformity as well as contaminations were analyzed in various tablets. Coating thickness and uniformity was characterized using Ti as an elemental marker. Additionally, Fe was detected as a contamination. In a follow-up work by Smith et al. [187], hyperspectral imaging was used to investigate minor elements present in

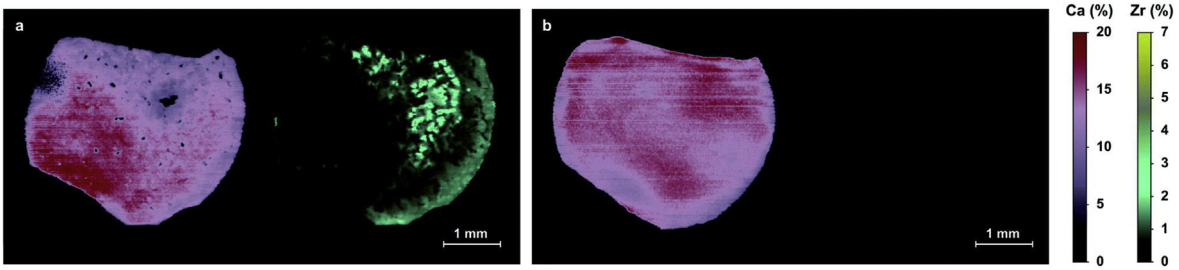

Fig. 10. LIBS transversal chemical imaging for Ca and Zr obtained on the two cross sections of a 3-mm wide fiber pulled at 6 mm h^{-1} and located at (a) z = 19 mm and (b) z = 27 mm [189]. Reproduced from by permission of The Royal Society of Chemistry, CrystEngComm. 21, Lead-free piezoelectric crystals grown by the micro-pulling down technique in the BaTiO3–CaTiO3–BaZrO3 system, P. Veber et al., 2019.

tablet coatings such as Na, Mg and K. Additionally, PCA was employed and successfully used for the classification of 4 different tablet coatings.

The capabilities of LIBS for the investigating the composition of solar cells was reported by Lee et al. [188]. In this work, the composition of a commercial Cu(In,Ga)Se2 solar cells module was mapped. Obtained results were in good agreement with conventionally used SIMS analysis making LIBS a promising tool in quality control in the solar cells industries as analysis times could be reduced significantly.

In the work of Veber et al. LIBS was used as an analytical tool to investigate elemental distributions of Ca and Zr in lead-free piezoelectric crystals grown by the micro-pulling down technique [189]. Longitudinal LIBS analysis was in good agreement with EPMA analysis and was able to reveal inhomogeneities of Zr especially at high pulling speeds. Additionally, cross-sections of pulled fibres revealed elemental segregation at the core (Fig. 10).

5. Conclusion

LIBS is gaining more and more attention in the field of elemental imaging, mainly due to its ease of use in terms of sample preparation, speed of analysis and simple instrumentation compared to similar techniques. However, recently these advantages have become also accessible with LA-ICP-MS using laser-ablations systems with fast washout cells and modern ICP-TOF-MS instrumentation. Nevertheless, compared to this advanced approach LIBS offers some unique benefits such as access to the whole periodic table of elements and the possibility to collect elemental and molecular information simultaneously. In addition, LIBS instrumentation is usually significantly cheaper than LA-ICP-MS Thus, applications become feasible which could not be addressed with other elemental imaging techniques, some prominent examples have been presented within this review.

Despite the general applicability of LIBS there are still some limitations which hamper the usefulness for challenging research tasks. In particular, to fully exploit the multi-element capabilities of this technique the measurement of broadband spectra is obligatory. However, to ensure selective analysis the presence of spectral interferences must be avoided, necessitating also requirements regarding spectral resolution. Unfortunately, most instruments enable either the collection of broadband spectra with rather low resolution or the analysis of small wavelength sections with high resolution. Consequently, the development of LIBS spectrometer which enable the simultaneous measurement of the whole spectral range (approximately from 200 to 1000 nm) with high resolution is aimed for.

Another weakness of current LIBS instrumentation is the sometimes insufficient sensitivity, thus measurements require the use of increased laser beam diameters to enable reliable analyte detection, and thereby imaging applications which need a high spatial resolution are disabled. A common solution to improve the sensitivity of analysis is the use of ICCD detectors or novel developments such as sCMOS detectors, enabling LIBS measurements with significantly improved detection limits. But usually with these advanced detectors only a certain spectral range can be covered, disabling the coincident detection of emission lines from different wavelength ranges. Even though, recording of high-resolution LIBS spectra with excellent sensitivity can be already achieved by combining an Echelle spectrometer with several ICCD detection units, ongoing improvements in LIBS instrumentation are demanded which will most probably allow for higher sensitivity at a lower price point in the future.

Besides instrumental developments, novel approaches such as Tandem LA-ICP-MS/LIBS, LIBS/Raman or double-or multi-pulse LIBS are promising to enhance the performance of LIBS [190] as well. In the case of Tandem LA-ICP-MS/LIBS, trace elements can be detected with the high sensitivity of ICP-MS and LIBS is used for the analysis of minor and major components as well as e.g. H, C, N and O making it a very versatile tool for multi-element imaging. The applicability of this Tandem approach for the investigation of tissue thin cuts [113] and archaeological samples [167] have been published recently. Hybrid LIBS/Raman systems have been recently reported in literature [191]. With this setup complementary information obtained from Raman spectroscopy was combined with LIBS data and used e.g. to improve classification of polymers [192] and analysis of forensic samples such as pigments and inks [193]. This combination is very promising to solve difficult classification tasks which seem to become more and more important. Double-pulse LIBS uses two consecutive laser pulses increasing the plasma temperature and reducing the atmospheric pressure and number density. This approach is especially interesting for applications which demand quasi non-destructive sample analysis such as valuable art work or heritage samples. With the use of a fs-laser for the ablation step only a minimum of sample material is consumed, which is efficiently atomized and excited with the second pulse from a ns-laser. This allows in particular significant improvements in the spatial resolution of analysis as a result of the enhanced sensitivity [120,138].

The progress of various chemometric approaches useful for LIBS data evaluation is also remarkable and may help advancing the establishment of LIBS as an elemental imaging technique, which is also capable of chemical sample classification. Here, especially the advantage of broadband LIBS spectra should be mentioned. Improvements of automatic peak detection combined with multivariate evaluation methods may enable fast and superior data evaluation strategies taking advantage of the information present in broadband LIBS spectra compared to simple univariate evaluations where only one emission signal from the spectrum is used. Nevertheless, due to the fast advancements in multivariate data evaluation strategies such as machine learning, algorithms are often used as black-boxes, often leading to misinterpretation of results. Therefore, expertise in this field could be very valuable for LIBS.

At the same time, some aspects of LIBS elemental mapping – most notably quantification - remain to be challenging. In this field, novel approaches such as multivariate calibration or calibration-free quantitation may prove to be useful tools.

Declaration of competing interest

The authors declare that they have no known competing financial interests or personal relationships that could have appeared to influence the work reported in this paper.

Acknowledgments

A. Limbeck and L. Brunnbauer gratefully acknowledges the funding by the Austrian Research Promotion Agency (FFG, Project No. 863947). P. Janovszky, A. Kéri and G. Galbács kindly acknowledge the financial support received from various sources including the Ministry of Innovation and Technology (through projects No. TUDFO/47138–1/2019-ITM FIKP) and the National Research, Development and Innovation Office (through projects No. K_129063, EFOP-3.6.2-16-2017-00005, GINOP-2.3.3-15-2016-00040 and TKP 2020 Thematic Excellence Program 2020) of Hungary. P. Modlitbová, P. Pořízka and J. Kaiser gratefully acknowledge the support by the Ministry of Education, Youth and Sports of the Czech Republic under the project CEITEC 2020 (LQ1601) and the Czech Grant Agency under the project GACR Junior (20-19526Y).

References

[1] G. Friedbacher, H. Bubert, Surface and Thin Film Analysis: A Compendium of Principles, Instrumentation, and Applications, John Wiley & Sons, 2011.

[2] R.E. Russo, X. Mao, H. Liu, J. Gonzalez, S.S. Mao, Laser ablation in analytical chemistry—a review, Talanta 57 (2002) 425–451, https://doi.org/10.1016/S0039-9140(02)00053-X.

[3] A. Limbeck, M. Bonta, W. Nischkauer, Improvements in the direct analysis of advanced materials using ICP-based measurement techniques, J. Anal. At. Spectrom. 32 (2017) 212–232, https://doi.org/10.1039/C6JA00335D.

[4] A. Limbeck, P. Galler, M. Bonta, G. Bauer, W. Nischkauer, F. Vanhaecke, Recent advances in quantitative LA-ICP-MS analysis: challenges and solutions in the life sciences and environmental chemistry, Anal. Bioanal. Chem. 407 (2015) 6593–6617, https://doi.org/10.1007/s00216-015-8858-0.

[5] M.E. Shaheen, J.E. Gagnon, B.J. Fryer, Femtosecond (fs) lasers coupled with modern ICP-MS instruments provide new and improved potential for in situ elemental and isotopic analyses in the geosciences, Chem. Geol. 330–331 (2012) 260–273, https://doi.org/10.1016/j.chemgeo.2012.09.016.

[6] D.A. Cremers, L.J. Radziemski, Handbook of Laser-Induced Breakdown Spectroscopy, John Wiley & Sons, 2013.

[7] A.W. Miziolek, V. Palleschi, I. Schechter, Laser Induced Breakdown Spectroscopy, Cambridge University Press, 2006.

[8] J.M. Vadillo, S. Palanco, M.D. Romero, J.J. Laserna, Applications of laser-induced breakdown spectrometry (LIBS) in surface analysis, Fresenius' J. Anal. Chem. 355 (1996) 909–912, https://doi.org/10.1007/s0021663550909.

[9] T. Kim, C.T. Lin, Y. Yoon, Compositional mapping by laser-induced breakdown spectroscopy, J. Phys. Chem. B 102 (1998) 4284–4287, https://doi.org/10.1021/jp980245m.

[10] V. Piñon, M.P. Mateo, G. Nicolas, Laser-induced breakdown spectroscopy for chemical mapping of materials, Appl. Spectrosc. Rev. 48 (2013) 357–383, https://doi.org/10.1080/05704928.2012.717569.

[11] H. Bette, R. Noll, High speed laser-induced breakdown spectrometry for scanning microanalysis, J. Phys. Appl. Phys. 37 (2004) 1281–1288, https://doi.org/10.1088/0022-3727/37/8/018.

[12] D. Menut, P. Fichet, J.-L. Lacour, A. Rivoallan, P. Mauchien, Micro-laser-induced breakdown spectroscopy technique: a powerful method for performing quantitative surface mapping on conductive and nonconductive samples, Appl. Optic. 42 (2003) 6063–6071, https://doi.org/10.1364/AO.42.006063.

[13] L. Jolivet, M. Leprince, S. Moncayo, L. Sorbier, C.-P. Lienemann, V. Motto-Ros, Review of the recent advances and applications of LIBS-based imaging, Spectrochim. Acta Part B At. Spectrosc. 151 (2019) 41–53, https://doi.org/10.1016/j.sab.2018.11.008.

[14] S.J.M.V. Malderen, A.J. Managh, B.L. Sharp, F. Vanhaecke, Recent developments in the design of rapid response cells for laser ablation-inductively coupled plasma-mass spectrometry and their impact on bio-imaging applications, J. Anal. At. Spectrom. 31 (2016) 423–439, https://doi.org/10.1039/C5JA00430F.

[15] C.C. Garcia, H. Lindner, K. Niemax, Transport efficiency in femtosecond laser ablation inductively coupled plasma mass spectrometry applying ablation cells with short and long washout times, Spectrochim. Acta Part B At. Spectrosc. 62 (2007) 13–19, https://doi.org/10.1016/j.sab.2006.11.005.

[16] A.A. Bol'shakov, X. Mao, J.J. González, R.E. Russo, Laser ablation molecular isotopic spectrometry (LAMIS): current state of the art, J. Anal. At. Spectrom. 31 (2016) 119–134, https://doi.org/10.1039/C5JA00310E.

[17] J.D. Woodhead, M.S.A. Horstwood, J.M. Cottle, Advances in isotope ratio determination by LA–ICP–MS, Elements 12 (2016) 317–322, https://doi.org/10.2113/gselements.12.5.317.

[18] F.J. Fortes, J. Moros, P. Lucena, L.M. Cabalín, J.J. Laserna, Laser-induced breakdown spectroscopy, Anal. Chem. 85 (2013) 640–669, https://doi.org/10.1021/ac303220r.

[19] D.W. Hahn, N. Omenetto, Laser-induced breakdown spectroscopy (LIBS), Part II: review of instrumental and methodological approaches to material analysis and applications to different fields, Appl. Spectrosc. 66 (2012) 347–419, https://doi.org/10.1366/11-06574.

[20] G. Galbács, A critical review of recent progress in analytical laser-induced breakdown spectroscopy, Anal. Bioanal. Chem. 407 (2015) 7537–7562, https://doi.org/10.1007/s00216-015-8855-3.

[21] C. Pasquini, J. Cortez, L.M.C. Silva, F.B. Gonzaga, Laser induced breakdown spectroscopy, J. Braz. Chem. Soc. 18 (2007) 463–512, https://doi.org/10.1590/S0103-50532007000300002.

[22] J. Laserna, J.M. Vadillo, P. Purohit, Laser-induced breakdown spectroscopy (LIBS): fast, effective, and agile leading edge analytical technology, Appl. Spectrosc. 72 (2018) 35–50, https://doi.org/10.1177/0003702818791926.

[23] S. Musazzi, U. Perini, LIBS instrumental techniques, in: S. Musazzi, U. Perini (Eds.), Laser-Induc. Breakdown Spectrosc. Theory Appl., Springer, Berlin, Heidelberg, 2014, pp. 59–89, https://doi.org/10.1007/978-3-642-45085-3_3.

[24] R. Noll, Laser-induced breakdown spectroscopy, in: R. Noll (Ed.), Laser-Induc. Breakdown Spectrosc. Fundam. Appl., Springer, Berlin, Heidelberg, 2012, pp. 7–15, https://doi.org/10.1007/978-3-642-20668-9_2.

[25] J.P. Singh, S.N. Thakur, Laser-Induced Breakdown Spectroscopy, Elsevier, 2007.

[26] W. Shi, Q. Fang, X. Zhu, R.A. Norwood, N. Peyghambarian, Fiber lasers and their applications [Invited], Appl. Optic. 53 (2014) 6554–6568, https://doi.org/10.1364/AO.53.006554.

[27] T.A. Labutin, V.N. Lednev, A.A. Ilyin, A.M. Popov, Femtosecond laser-induced breakdown spectroscopy, J. Anal. At. Spectrom. 31 (2016) 90–118, https://doi.org/10.1039/C5JA00301F.

[28] Y. Li, D. Tian, Y. Ding, G. Yang, K. Liu, C. Wang, X. Han, A review of laser-induced breakdown spectroscopy signal enhancement, Appl. Spectrosc. Rev. 53 (2018) 1–35, https://doi.org/10.1080/05704928.2017.1352509.

[29] G. Galbács, V. Budavári, Z. Geretovszky, Multi-pulse laser-induced plasma spectroscopy using a single laser source and a compact spectrometer, J. Anal. At. Spectrom. 20 (2005) 974–980, https://doi.org/10.1039/B504373E.

[30] N. Jedlinszki, G. Galbács, An evaluation of the analytical performance of collinear multi-pulse laser induced breakdown spectroscopy, Microchem. J. 97 (2011) 255–263, https://doi.org/10.1016/j.microc.2010.09.009.

[31] G. Galbács, N. Jedlinszki, K. Herrera, N. Omenetto, B.W. Smith, J.D. Winefordner, A study of ablation, spatial, and temporal characteristics of laser-induced plasmas generated by multiple collinear pulses, Appl. Spectrosc. 64 (2010) 161–172, https://doi.org/10.1366/000370210790619609.

[32] V.I. Babushok, F.C. DeLucia, J.L. Gottfried, C.A. Munson, A.W. Miziolek, Double pulse laser ablation and plasma: laser induced breakdown spectroscopy signal enhancement, Spectrochim. Acta Part B At. Spectrosc. 61 (2006) 999–1014, https://doi.org/10.1016/j.sab.2006.09.003.

[33] J. Scaffidi, S.M. Angel, D.A. Cremers, Emission Enhancement Mechanisms in Dual-Pulse LIBS, ACS Publications, 2006.

[34] C. Schiavo, L. Menichetti, E. Grifoni, S. Legnaioli, G. Lorenzetti, F. Poggialini, S. Pagnotta, V. Palleschi, High-resolution three-dimensional compositional imaging by double-pulse laser-induced breakdown spectroscopy, J. Instrum. 11 (2016), https://doi.org/10.1088/1748-0221/11/08/C08002. C08002–C08002.

[35] D. Prochazka, T. Zikmund, P. Pořízka, A. Břínek, J. Klus, J. Šalplachta, J. Kynický, J. Novotný, J. Kaiser, Joint utilization of double-pulse laser-induced breakdown spectroscopy and X-ray computed tomography for volumetric information of geological samples, J. Anal. At. Spectrom. 33 (2018) 1993–1999, https://doi.org/10.1039/C8JA00232K.

[36] R. Grassi, E. Grifoni, S. Gufoni, S. Legnaioli, G. Lorenzetti, N. Macro, L. Menichetti, S. Pagnotta, F. Poggialini, C. Schiavo, V. Palleschi, Three-dimensional compositional mapping using double-pulse micro-laser-induced breakdown spectroscopy technique, Spectrochim. Acta Part B At. Spectrosc. 127 (2017) 1–6, https://doi.org/10.1016/j.sab.2016.11.004.

[37] J. Klus, P. Mikysek, D. Prochazka, P. Pořízka, P. Prochazková, J. Novotný, T. Trojek, K. Novotný, M. Slobodník, J. Kaiser, Multivariate approach to the chemical mapping of uranium in sandstone-hosted uranium ores analyzed using double pulse Laser-Induced Breakdown Spectroscopy, Spectrochim. Acta Part B At. Spectrosc. 123 (2016) 143–149, https://doi.org/10.1016/j.sab.2016.08.014.

[38] V. Zorba, X. Mao, R.E. Russo, Ultrafast laser induced breakdown spectroscopy for high spatial resolution chemical analysis, Spectrochim. Acta Part B At. Spectrosc. 66 (2011) 189–192, https://doi.org/10.1016/j.sab.2010.12.008.

[39] A.S. Eppler, D.A. Cremers, D.D. Hickmott, M.J. Ferris, A.C. Koskelo, Matrix effects in the detection of Pb and Ba in soils using laser-induced breakdown spectroscopy, Appl. Spectrosc. 50 (1996) 1175–1181, https://doi.org/10.1366/0003702963905123.

[40] K.T. Rodolfa, D.A. Cremers, Capabilities of surface composition analysis using a long laser-induced breakdown spectroscopy spark, Appl. Spectrosc. 58 (2004) 367–375, https://doi.org/10.1366/000370204773580185.

[41] V. Sturm, Optical micro-lens array for laser plasma generation in spectrochemical analysis, J. Anal. At. Spectrom. 22 (2007) 1495–1500, https://doi.org/10.1039/B708564H.

[42] A.J. Effenberger, J.R. Scott, Effect of atmospheric conditions on LIBS spectra, Sensors 10 (2010) 4907–4925, https://doi.org/10.3390/s100504907.

[43] C.C. García, M. Corral, J.M. Vadillo, J.J. Laserna, Angle-resolved laser-induced breakdown spectrometry for depth profiling of coated materials, Appl. Spectrosc. 54 (2000) 1027–1031, https://doi.org/10.1366/0003702001950526.

[44] P. Modlitbová, P. Pořízka, J. Kaiser, Laser-induced breakdown spectroscopy as a promising tool in the elemental bioimaging of plant tissues, TrAC Trends Anal. Chem. (Reference Ed.) 122 (2020), 115729, https://doi.org/10.1016/j.trac.2019.115729.

[45] B. Busser, S. Moncayo, J.-L. Coll, L. Sancey, V. Motto-Ros, Elemental imaging using laser-induced breakdown spectroscopy: a new and promising approach for biological and medical applications, Coord. Chem. Rev. 358 (2018) 70–79, https://doi.org/10.1016/j.ccr.2017.12.006.

[46] J.S. Becker, A. Matusch, B. Wu, Bioimaging mass spectrometry of trace elements – recent advance and applications of LA-ICP-MS: a review, Anal. Chim. Acta 835 (2014) 1–18, https://doi.org/10.1016/j.aca.2014.04.048.

[47] W. Li, X. Li, X. Li, Z. Hao, Y. Lu, X. Zeng, A review of remote laser-induced breakdown spectroscopy, Appl. Spectrosc. Rev. 55 (2020) 1–25, https://doi.org/10.1080/05704928.2018.1472102.

[48] P.D. Barnett, N. Lamsal, S.M. Angel, Standoff laser-induced breakdown spectroscopy (LIBS) using a miniature wide field of view spatial heterodyne spectrometer with sub-microsteradian collection optics, Appl. Spectrosc. 71 (2017) 583–590, https://doi.org/10.1177/0003702816687569.

[49] I.B. Gornushkin, B.W. Smith, U. Panne, N. Omenetto, Laser-induced breakdown spectroscopy combined with spatial heterodyne spectroscopy, Appl. Spectrosc. 68 (2014) 1076–1084, https://doi.org/10.1366/14-07544.

[50] A.B. Gojani, D.J. Palásti, A. Paul, G. Galbács, I.B. Gornushkin, Analysis and

classification of liquid samples using spatial heterodyne Raman spectroscopy, Appl. Spectrosc. 73 (2019) 1409–1419, https://doi.org/10.1177/0003702819863847.
[51] T. Zhang, H. Tang, H. Li, Chemometrics in laser-induced breakdown spectroscopy, J. Chemom. 32 (2018), e2983, https://doi.org/10.1002/cem.2983.
[52] S. Moncayo, L. Duponchel, N. Mousavipak, G. Panczer, F. Trichard, B. Bousquet, F. Pelascini, V. Motto-Ros, Exploration of megapixel hyperspectral LIBS images using principal component analysis, J. Anal. At. Spectrom. 33 (2018) 210–220, https://doi.org/10.1039/C7JA00398F.
[53] D.L. Blaney, R.C. Wiens, S. Maurice, S.M. Clegg, R.B. Anderson, L.C. Kah, S.L. Mouélic, A. Ollila, N. Bridges, R. Tokar, G. Berger, J.C. Bridges, A. Cousin, B. Clark, M.D. Dyar, P.L. King, N. Lanza, N. Mangold, P.-Y. Meslin, H. Newsom, S. Schröder, S. Rowland, J. Johnson, L. Edgar, O. Gasnault, O. Forni, M. Schmidt, W. Goetz, K. Stack, D. Sumner, M. Fisk, M.B. Madsen, Chemistry and texture of the rocks at Rocknest, Gale Crater: evidence for sedimentary origin and diagenetic alteration, J. Geophys. Res. Planets. 119 (2014) 2109–2131, https://doi.org/10.1002/2013JE004590.
[54] J. Yan, S. Li, K. Liu, R. Zhou, W. Zhang, Z. Hao, X. Li, D. Wang, Q. Li, X. Zeng, An image features assisted line selection method in laser-induced breakdown spectroscopy, Anal. Chim. Acta 1111 (2020) 139–146, https://doi.org/10.1016/j.aca.2020.03.030.
[55] C. Harris, M. Stephens, A combined corner and edge detector, in: Proc Fourth Alvey Vis. Conf, 1988, pp. 147–152.
[56] P. Pořízka, J. Klus, A. Hrdlička, J. Vrábel, P. Škarková, D. Prochazka, J. Novotný, K. Novotný, J. Kaiser, Impact of Laser-Induced Breakdown Spectroscopy data normalization on multivariate classification accuracy, J. Anal. At. Spectrom. 32 (2017) 277–288, https://doi.org/10.1039/C6JA00322B.
[57] E. Képeš, P. Pořízka, J. Klus, P. Modlitbová, J. Kaiser, Influence of baseline subtraction on laser-induced breakdown spectroscopic data, J. Anal. At. Spectrom. 33 (2018) 2107–2115, https://doi.org/10.1039/C8JA00209F.
[58] M. Bonta, H. Lohninger, M. Marchetti-Deschmann, A. Limbeck, Application of gold thin-films for internal standardization in LA-ICP-MS imaging experiments, Analyst 139 (2014) 1521–1531, https://doi.org/10.1039/c3an01511d.
[59] A.A. Green, M. Berman, P. Switzer, M.D. Craig, A transformation for ordering multispectral data in terms of image quality with implications for noise removal, IEEE Trans. Geosci. Rem. Sens. 26 (1988) 65–74, https://doi.org/10.1109/36.3001.
[60] P. Pořízka, J. Klus, E. Képeš, D. Prochazka, D.W. Hahn, J. Kaiser, On the utilization of principal component analysis in laser-induced breakdown spectroscopy data analysis, a review, Spectrochim. Acta Part B At. Spectrosc. 148 (2018) 65–82, https://doi.org/10.1016/j.sab.2018.05.030.
[61] S. Romppanen, H. Häkkänen, S. Kaski, Singular value decomposition approach to the yttrium occurrence in mineral maps of rare earth element ores using laser-induced breakdown spectroscopy, Spectrochim. Acta Part B At. Spectrosc. 134 (2017) 69–74, https://doi.org/10.1016/j.sab.2017.06.002.
[62] I.T. Jolliffe, Principal component analysis, Technometrics 45 (2003) 276.
[63] A. Limbeck, DS013 concrete, n.d. http://www.imagelab.at/en_data_repository.html. (Accessed 30 June 2020).
[64] K. Fukunaga, Introduction to Statistical Pattern Classification, academic press, San Diego Calif. USA, 1990.
[65] D.L. Massart, B.G. Vandeginste, L.M. Buydens, P.J. Lewi, J. Smeyers-Verbeke, S.D. Jong, Handbook of Chemometrics and Qualimetrics, Elsevier Science Inc., 1998.
[66] G.N. Lance, W.T. Williams, A general theory of classificatory sorting Strategies1. Hierarchical systems, Comput. J. 9 (1967) 373–380, https://doi.org/10.1093/comjnl/9.4.373.
[67] J.H. Ward, Hierarchical grouping to optimize an objective function, J. Am. Stat. Assoc. 58 (1963) 236–244, https://doi.org/10.1080/01621459.1963.10500845.
[68] H. Lohninger, Similarity map, help page of epina ImageLab, Release 3.20, (n.d.), http://www.imagelab.at/help/similarity_map.htm. (Accessed 30 June 2020).
[69] M. Zürcher, J.T. Clerc, M. Farkas, E. Pretsch, General theory of similarity measures for library search systems, Anal. Chim. Acta 206 (1988) 161–172, https://doi.org/10.1016/S0003-2670(00)80839-9.
[70] P.C. Mahalanobis, On the generalized distance in statistics, in: National Institute of Science of India, 1936.
[71] F.A. Kruse, A.B. Lefkoff, J.W. Boardman, K.B. Heidebrecht, A.T. Shapiro, P.J. Barloon, A.F.H. Goetz, The spectral image processing system (SIPS)-interactive visualization and analysis of imaging spectrometer data, AIP Conf. Proc. 283 (1993) 192–201, https://doi.org/10.1063/1.44433.
[72] Y. Du, C.-I. Chang, H. Ren, C.-C. Chang, J.O. Jensen, F.M. D'Amico, New hyperspectral discrimination measure for spectral characterization, Opt. Eng. 43 (2004) 1777–1786, https://doi.org/10.1117/1.1766301.
[73] J.M.P. Nascimento, J.M.B. Dias, Vertex component analysis: a fast algorithm to unmix hyperspectral data, IEEE Trans. Geosci. Rem. Sens. 43 (2005) 898–910, https://doi.org/10.1109/TGRS.2005.844293.
[74] T. Kohonen, Self-organized formation of topologically correct feature maps, Biol. Cybern. 43 (1982) 59–69, https://doi.org/10.1007/BF00337288.
[75] S. Pagnotta, M. Lezzerini, B. Campanella, G. Gallello, E. Grifoni, S. Legnaioli, G. Lorenzetti, F. Poggialini, S. Raneri, A. Safi, V. Palleschi, Fast quantitative elemental mapping of highly inhomogeneous materials by micro-Laser-Induced Breakdown Spectroscopy, Spectrochim. Acta Part B At. Spectrosc. 146 (2018) 9–15, https://doi.org/10.1016/j.sab.2018.04.018.
[76] Y. Tang, Y. Guo, Q. Sun, S. Tang, J. Li, L. Guo, J. Duan, Industrial polymers classification using laser-induced breakdown spectroscopy combined with self-organizing maps and K-means algorithm, Optik 165 (2018) 179–185.
[77] J. Klus, P. Pořízka, D. Prochazka, P. Mikysek, J. Novotný, K. Novotný, M. Slobodník, J. Kaiser, Application of self-organizing maps to the study of U-Zr-Ti-Nb distribution in sandstone-hosted uranium ores, Spectrochim. Acta Part B at, Spectroscopy (Glos.) 131 (2017) 66–73, https://doi.org/10.1016/j.sab.2017.03.008.
[78] G.J. McLachlan, Discriminant Analysis and Statistical Pattern Recognition, Wiley, N. Y., 1992.
[79] L. Chuen Lee, C.-Y. Liong, A. Aziz Jemain, Partial least squares-discriminant analysis (PLS-DA) for classification of high-dimensional (HD) data: a review of contemporary practice strategies and knowledge gaps, Analyst 143 (2018) 3526–3539, https://doi.org/10.1039/C8AN00599K.
[80] S. Wold, M. Sjöström, L. Eriksson, PLS-regression: a basic tool of chemometrics, Chemometr. Intell. Lab. Syst. 58 (2001) 109–130, https://doi.org/10.1016/S0169-7439(01)00155-1.
[81] L. Breiman, Random forests, Mach. Learn. 45 (2001) 5–32.
[82] L. Breiman, A. Cutler, Random forest. https://www.stat.berkeley.edu/~breiman/RandomForests/cc_home.htm, 2020. (Accessed 29 June 2020).
[83] L. Pagnin, L. Brunnbauer, R. Wiesinger, A. Limbeck, M. Schreiner, Multivariate analysis and laser-induced breakdown spectroscopy (LIBS): a new approach for the spatially resolved classification of modern art materials, Anal. Bioanal. Chem. (2020), https://doi.org/10.1007/s00216-020-02574-z.
[84] L. Brunnbauer, S. Larisegger, H. Lohninger, M. Nelhiebel, A. Limbeck, Spatially resolved polymer classification using laser induced breakdown spectroscopy (LIBS) and multivariate statistics, Talanta (2019), 120572, https://doi.org/10.1016/j.talanta.2019.120572.
[85] D. Livingstone, A Practical Guide to Scientific Data Analysis, Wiley Online Library, 2009.
[86] R.E. Bellman, Adaptive Control Processes: A Guided Tour, Princeton University Press, 2015.
[87] V. Vapnik, Pattern recognition using generalized portrait method, Autom, Remote Control 24 (1963) 774–780.
[88] A.J. Smola, B. Schölkopf, A tutorial on support vector regression, Stat. Comput. 14 (2004) 199–222, https://doi.org/10.1023/B:STCO.0000035301.49549.88.
[89] X. Li, S. Yang, R. Fan, X. Yu, D. Chen, Discrimination of soft tissues using laser-induced breakdown spectroscopy in combination with k nearest neighbors (kNN) and support vector machine (SVM) classifiers, Optic Laser. Technol. 102 (2018) 233–239, https://doi.org/10.1016/j.optlastec.2018.01.028.
[90] K.-L. Du, M.N. Swamy, Neural Networks and Statistical Learning, Springer Science & Business Media, 2013.
[91] J. El Haddad, M. Villot-Kadri, A. Ismaël, G. Gallou, K. Michel, D. Bruyère, V. Laperche, L. Canioni, B. Bousquet, Artificial neural network for on-site quantitative analysis of soils using laser induced breakdown spectroscopy, Spectrochim. Acta Part B At. Spectrosc. 79–80 (2013) 51–57, https://doi.org/10.1016/j.sab.2012.11.007.
[92] A. Koujelev, S.-L. Lui, Artificial neural networks for material identification, mineralogy and analytical geochemistry based on laser-induced breakdown spectroscopy, Artif. NEURAL Netw. Ind. Ctrl. Eng. Appl. (2011) 91.
[93] S. Pagnotta, M. Lezzerini, B. Campanella, S. Legnaioli, F. Poggialini, V. Palleschi, A new approach to non-linear multivariate calibration in laser-induced breakdown spectroscopy analysis of silicate rocks, Spectrochim. Acta Part B At. Spectrosc. 166 (2020), 105804, https://doi.org/10.1016/j.sab.2020.105804.
[94] H.K. Sanghapi, J. Jain, A. Bol'shakov, C. Lopano, D. McIntyre, R. Russo, Determination of elemental composition of shale rocks by laser induced breakdown spectroscopy, Spectrochim. Acta Part B At. Spectrosc. 122 (2016) 9–14, https://doi.org/10.1016/j.sab.2016.05.011.
[95] T. Hastie, R. Tibshirani, J. Friedman, The Elements of Statistical Learnin, Springer, New York, 2009.
[96] T. Wang, L. Jiao, C. Yan, Y. He, M. Li, T. Zhang, H. Li, Simultaneous quantitative analysis of four metal elements in oily sludge by laser induced breakdown spectroscopy coupled with wavelet transform-random forest (WT-RF), Chemometr. Intell. Lab. Syst. 194 (2019), 103854, https://doi.org/10.1016/j.chemolab.2019.103854.
[97] W.A.C. Hallada, Image sharpening for mixed spatial and spectral resolution satellite systems, May 09, 1983 - May 13, 1983, https://ntrs.nasa.gov/search.jsp?R=19850028100, 1983. (Accessed 29 June 2020).
[98] M.G.-A.C. author, X. Otazu, O. Fors, A. Seco, Comparison between Mallat's and the 'à trous' discrete wavelet transform based algorithms for the fusion of multispectral and panchromatic images, Int. J. Rem. Sens. 26 (2005) 595–614, https://doi.org/10.1080/01431160512331314056.
[99] A. Sussulini, J.S. Becker, J.S. Becker, Laser ablation ICP-MS: application in biomedical research, Mass Spectrom. Rev. 36 (2017) 47–57, https://doi.org/10.1002/mas.21481.
[100] J. Sabine Becker, Imaging of metals in biological tissue by laser ablation inductively coupled plasma mass spectrometry (LA–ICP–MS): state of the art and future developments, J. Mass Spectrom. 48 (2013) 255–268.
[101] B. Wu, J.S. Becker, Imaging techniques for elements and element species in plant science, Metallomics 4 (2012) 403–416.
[102] J. Kaiser, K. Novotný, M.Z. Martin, A. Hrdlička, R. Malina, M. Hartl, V. Adam, R. Kizek, Trace elemental analysis by laser-induced breakdown spectroscopy—biological applications, Surf. Sci. Rep. 67 (2012) 233–243.
[103] D. Santos, L.C. Nunes, G.G.A. De Carvalho, M.d.S. Gomes, P.F. De Souza,

F.d.O. Leme, L.G.C. Dos Santos, F.J. Krug, Laser-induced breakdown spectroscopy for analysis of plant materials: a review, Spectrochim. Acta, Part B 71 (2012) 3–13.
[104] G.S. Senesi, J. Cabral, C.R. Menegatti, B. Marangoni, G. Nicolodelli, Recent advances and future trends in LIBS applications to agricultural materials and their food derivatives: an overview of developments in the last decade (2010–2019). Part II. Crop plants and their food derivatives, TrAC Trends Anal. Chem. (Reference Ed.) 118 (2019) 453–469.
[105] B. Sezer, G. Bilge, I.H. Boyaci, Capabilities and limitations of LIBS in food analysis, TrAC Trends Anal. Chem. (Reference Ed.) 97 (2017) 345–353.
[106] R. Gaudiuso, N. Melikechi, Z.A. Abdel-Salam, M.A. Harith, V. Palleschi, V. Motto-Ros, B. Busser, Laser-induced breakdown spectroscopy for human and animal health: a review, Spectrochim. Acta Part B At. Spectrosc. 152 (2019) 123–148.
[107] P. Pořízka, P. Prochazková, D. Prochazka, L. Sládková, J. Novotný, M. Petrilak, M. Brada, O. Samek, Z. Pilát, P. Zemánek, Algal biomass analysis by laser-based analytical techniques—a review, Sensors 14 (2014) 17725–17752.
[108] S.J. Rehse, A review of the use of laser-induced breakdown spectroscopy for bacterial classification, quantification, and identification, Spectrochim. Acta Part B At. Spectrosc. 154 (2019) 50–69.
[109] M. Martinez, M. Baudelet, Calibration strategies for elemental analysis of biological samples by LA-ICP-MS and LIBS—A review, Anal. Bioanal. Chem. (2020) 1–10.
[110] S.C. Jantzi, V. Motto-Ros, F. Trichard, Y. Markushin, N. Melikechi, A. De Giacomo, Sample treatment and preparation for laser-induced breakdown spectroscopy, Spectrochim. Acta Part B At. Spectrosc. 115 (2016) 52–63.
[111] G.G.A. de Carvalho, M.B.B. Guerra, A. Adame, C.S. Nomura, P.V. Oliveira, H.W.P. de Carvalho, D. Santos, L.C. Nunes, F.J. Krug, Recent advances in LIBS and XRF for the analysis of plants, J. Anal. At. Spectrom. 33 (2018) 919–944.
[112] M. Bonta, S. Török, B. Hegedus, B. Döme, A. Limbeck, A comparison of sample preparation strategies for biological tissues and subsequent trace element analysis using LA-ICP-MS, Anal. Bioanal. Chem. 409 (2017) 1805–1814.
[113] M. Bonta, J.J. Gonzalez, C. Derrick Quarles, R.E. Russo, B. Hegedus, A. Limbeck, Elemental mapping of biological samples by the combined use of LIBS and LA-ICP-MS, J. Anal. At. Spectrom. 31 (2016) 252–258, https://doi.org/10.1039/C5JA00287G.
[114] L. Sancey, V. Motto-Ros, B. Busser, S. Kotb, J.M. Benoit, A. Piednoir, F. Lux, O. Tillement, G. Panczer, J. Yu, Laser spectrometry for multi-elemental imaging of biological tissues, Sci. Rep. 4 (2014) 6065.
[115] M. Martinez, C. Bayne, D. Aiello, M. Julian, R. Gaume, M. Baudelet, Multi-elemental matrix-matched calcium hydroxyapatite reference materials for laser ablation: evaluation on teeth by laser-induced breakdown spectroscopy, Spectrochim. Acta Part B At. Spectrosc. 159 (2019), 105650.
[116] V.K. Singh, A.K. Rai, P.K. Rai, P.K. Jindal, Cross-sectional study of kidney stones by laser-induced breakdown spectroscopy, Laser Med. Sci. 24 (2009) 749–759.
[117] E. Grifoni, S. Legnaioli, G. Lorenzetti, S. Pagnotta, F. Poggialini, V. Palleschi, From Calibration-Free to Fundamental Parameters Analysis: a comparison of three recently proposed approaches, Spectrochim. Acta Part B At. Spectrosc. 124 (2016) 40–46.
[118] P. Modlitbová, P. Pořízka, S. Střítežská, Š. Zezulka, M. Kummerová, K. Novotný, J. Kaiser, Detail investigation of toxicity, bioaccumulation, and translocation of Cd-based quantum dots and Cd salt in white mustard, Chemosphere 251 (2020), 126174.
[119] P.D. Ilhardt, J.R. Nuñez, E.H. Denis, J.J. Rosnow, E.J. Krogstad, R.S. Renslow, J.J. Moran, High-resolution elemental mapping of the root-rhizosphere-soil continuum using laser-induced breakdown spectroscopy (LIBS), Soil Biol. Biochem. 131 (2019) 119–132, https://doi.org/10.1016/j.soilbio.2018.12.029.
[120] P. Modlitbová, K. Novotný, P. Pořízka, J. Klus, P. Lubal, H. Zlámalová-Gargošová, J. Kaiser, Comparative investigation of toxicity and bioaccumulation of Cd-based quantum dots and Cd salt in freshwater plant Lemna minor L, Ecotoxicol. Environ. Saf. 147 (2018) 334–341.
[121] V.K. Singh, D.K. Tripathi, X. Mao, R.E. Russo, V. Zorba, Elemental mapping of lithium diffusion in doped plant leaves using laser-induced breakdown spectroscopy (LIBS), Appl. Spectrosc. 73 (2019) 387–394.
[122] Z. Xiande, C. Zhao, D. Xiaofan, D. Daming, Detecting and mapping harmful chemicals in fruit and vegetables using nanoparticle-enhanced laser-induced breakdown spectroscopy, Sci. Rep. Nat. Publ. Group. 9 (2019).
[123] C. Zhao, D. Dong, X. Du, W. Zheng, In-field, in situ, and in vivo 3-dimensional elemental mapping for plant tissue and soil analysis using laser-induced breakdown spectroscopy, Sensors 16 (2016) 1764.
[124] P. Modlitbová, A. Hlaváček, T. Švestková, P. Pořízka, L. Šimoníková, K. Novotný, J. Kaiser, The effects of photon-upconversion nanoparticles on the growth of radish and duckweed: bioaccumulation, imaging, and spectroscopic studies, Chemosphere 225 (2019) 723–734.
[125] J. Peng, Y. He, Z. Zhao, J. Jiang, F. Zhou, F. Liu, T. Shen, Fast visualization of distribution of chromium in rice leaves by re-heating dual-pulse laser-induced breakdown spectroscopy and chemometric methods, Environ. Pollut. 252 (2019) 1125–1132.
[126] J. Peng, Y. Sun, Q. Liu, Y. Yang, J. Zhou, W. Feng, X. Zhang, F. Li, Upconversion nanoparticles dramatically promote plant growth without toxicity, Nano Res 5 (2012) 770–782.
[127] Y. Gimenez, B. Busser, F. Trichard, A. Kulesza, J.M. Laurent, V. Zaun, F. Lux, J.M. Benoit, G. Panczer, P. Dugourd, O. Tillement, F. Pelascini, L. Sancey, V. Motto-Ros, 3D imaging of nanoparticle distribution in biological tissue by laser-induced breakdown spectroscopy, Sci. Rep. 6 (2016) 29936, https://doi.org/10.1038/srep29936.
[128] V. Motto-Ros, L. Sancey, Q.L. Ma, F. Lux, X.S. Bai, X.C. Wang, J. Yu, G. Panczer, O. Tillement, Mapping of native inorganic elements and injected nanoparticles in a biological organ with laser-induced plasma, Appl. Phys. Lett. 101 (2012), 223702.
[129] V. Motto-Ros, L. Sancey, X.C. Wang, Q.L. Ma, F. Lux, X.S. Bai, G. Panczer, O. Tillement, J. Yu, Mapping nanoparticles injected into a biological tissue using laser-induced breakdown spectroscopy, Spectrochim. Acta Part B At. Spectrosc. 87 (2013) 168–174.
[130] L. Sancey, S. Kotb, C. Truillet, F. Appaix, A. Marais, E. Thomas, Long-term in vivo clearance of gadolinium-based AGulX (Activation and Guiding of Irradiation by X-Ray) nanoparticles and their biocompatibility after systemic injection, ACS Nano 9 (2015) 2477–2488.
[131] A. Moussaron, S. Vibhute, A. Bianchi, S. Gündüz, S. Kotb, L. Sancey, V. Motto-Ros, S. Rizzitelli, Y. Crémillieux, F. Lux, Ultrasmall nanoplatforms as calcium-responsive contrast agents for magnetic resonance imaging, Small 11 (2015) 4900–4909.
[132] S. Kunjachan, A. Detappe, R. Kumar, T. Ireland, L. Cameron, D.E. Biancur, V. Motto-Ros, L. Sancey, S. Sridhar, G.M. Makrigiorgos, Nanoparticle mediated tumor vascular disruption: a novel strategy in radiation therapy, Nano Lett. 15 (2015) 7488–7496.
[133] A. Detappe, S. Kunjachan, L. Sancey, V. Motto-Ros, D. Biancur, P. Drane, R. Guieze, G.M. Makrigiorgos, O. Tillement, R. Langer, Advanced multimodal nanoparticles delay tumor progression with clinical radiation therapy, J. Contr. Release 238 (2016) 103–113.
[134] S. Moncayo, F. Trichard, B. Busser, M. Sabatier-Vincent, F. Pelascini, N. Pinel, I. Templier, J. Charles, L. Sancey, V. Motto-Ros, Multi-elemental imaging of paraffin-embedded human samples by laser-induced breakdown spectroscopy, Spectrochim. Acta Part B At. Spectrosc. 133 (2017) 40–44.
[135] A. Vogel, V. Venugopalan, Mechanisms of pulsed laser ablation of biological tissues, Chem. Rev. 103 (2003) 577–644.
[136] V.K. Singh, V. Kumar, J. Sharma, Importance of laser-induced breakdown spectroscopy for hard tissues (bone, teeth) and other calcified tissue materials, Laser Med. Sci. 30 (2015) 1763–1778, https://doi.org/10.1007/s10103-014-1549-9.
[137] M. Galiová, J. Kaiser, F.J. Fortes, K. Novotný, R. Malina, L. Prokeš, A. Hrdlička, T. Vaculovič, M.N. Fišáková, J. Svoboda, V. Kanický, J.J. Laserna, Multi-elemental analysis of prehistoric animal teeth by laser-induced breakdown spectroscopy and laser ablation inductively coupled plasma mass spectrometry, Appl. Optic. 49 (2010) C191–C199, https://doi.org/10.1364/AO.49.00C191.
[138] M. Galiová, J. Kaiser, K. Novotný, M. Ivanov, M. Nývltová Fišáková, L. Mancini, G. Tromba, T. Vaculovič, M. Liška, V. Kanický, Investigation of the osteitis deformans phases in snake vertebrae by double-pulse laser-induced breakdown spectroscopy, Anal. Bioanal. Chem. 398 (2010) 1095–1107, https://doi.org/10.1007/s00216-010-3976-1.
[139] Y. Markushin, N. Melikechi, Sensitive Detection of Epithelial Ovarian Cancer Biomarkers Using Tag-Laser Induced Breakdown Spectroscopy, Ovarian Cancer—Basic Sci. Perspect. Intech., 2012, pp. 153–170.
[140] N. Melikechi, Y. Markushin, Mono-and Multi-Element Coded Libs Assays and Methods, Google Patents, 2011.
[141] J.P. Robinson, B.P. Rajwa, V.P. Patsekin, E. Bae, Metal-antibody Tagging and Plasma-Based Detection, Google Patents, 2019.
[142] Z. Farka, T. Jurik, D. Kovář, L. Trnková, P. Skládal, Nanoparticle-based immunochemical biosensors and assays: recent advances and challenges, Chem. Rev. 117 (2017) 9973–10042.
[143] M. Konecna, K. Novotny, S. Krizkova, I. Blazkova, P. Kopel, J. Kaiser, P. Hodek, R. Kizek, V. Adam, Identification of quantum dots labeled metallothionein by fast scanning laser-induced breakdown spectroscopy, Spectrochim. Acta Part B At. Spectrosc. 101 (2014) 220–225.
[144] P. Modlitbová, Z. Farka, M. Pastucha, P. Pořízka, K. Novotný, P. Skládal, J. Kaiser, Laser-induced breakdown spectroscopy as a novel readout method for nanoparticle-based immunoassays, Microchim. Acta. 186 (2019) 629.
[145] C. Gondhalekar, E. Biela, B. Rajwa, E. Bae, V. Patsekin, J. Sturgis, C. Reynolds, I.-J. Doh, P. Diwakar, L. Stanker, Detection of E. coli labeled with metal-conjugated antibodies using lateral-flow assay and laser-induced breakdown spectroscopy, Anal. Bioanal. Chem. 412 (2020) 1291–1301.
[146] K. Rifai, F. Doucet, L. Özcan, F. Vidal, LIBS core imaging at kHz speed: Paving the way for real-time geochemical applications, Spectrochim. Acta Part B At. Spectrosc. 150 (2018) 43–48, https://doi.org/10.1016/j.sab.2018.10.007.
[147] J.O. Cáceres, F. Pelascini, V. Motto-Ros, S. Moncayo, F. Trichard, G. Panczer, A. Marín-Roldán, J.A. Cruz, I. Coronado, J. Martín-Chivelet, Megapixel multi-elemental imaging by Laser-Induced Breakdown Spectroscopy, a technology with considerable potential for paleoclimate studies, Sci. Rep. 7 (2017) 5080, https://doi.org/10.1038/s41598-017-05437-3.
[148] Q.L. Ma, V. Motto-Ros, W.Q. Lei, M. Boueri, L.J. Zheng, H.P. Zeng, M. Bar-Matthews, A. Ayalon, G. Panczer, J. Yu, Multi-elemental mapping of a speleothem using laser-induced breakdown spectroscopy, Spectrochim. Acta Part B At. Spectrosc. 65 (2010) 707–714, https://doi.org/10.1016/j.sab.2010.03.004.
[149] N. Hausmann, P. Siozos, A. Lemonis, A.C. Colonese, H.K. Robson, D. Anglos, Elemental mapping of Mg/Ca intensity ratios in marine mollusc shells using laser-induced breakdown spectroscopy, J. Anal. At. Spectrom. 32 (2017) 1467–1472, https://doi.org/10.1039/C7JA00131B.

[150] C. Fabre, D. Devismes, S. Moncayo, F. Pelascini, F. Trichard, A. Lecomte, B. Bousquet, J. Cauzid, V. Motto-Ros, Elemental imaging by laser-induced breakdown spectroscopy for the geological characterization of minerals, J. Anal. At. Spectrom. 33 (2018) 1345–1353, https://doi.org/10.1039/C8JA00048D.
[151] M. Gaft, Y. Raichlin, F. Pelascini, G. Panzer, V. Motto Ros, Imaging rare-earth elements in minerals by laser-induced plasma spectroscopy: molecular emission and plasma-induced luminescence, Spectrochim. Acta Part B At. Spectrosc. 151 (2019) 12–19, https://doi.org/10.1016/j.sab.2018.11.003.
[152] F. Trichard, S. Moncayo, D. Devismes, F. Pelascini, J. Maurelli, A. Feugier, C. Sasseville, F. Surma, V. Motto-Ros, Evaluation of a compact VUV spectrometer for elemental imaging by laser-induced breakdown spectroscopy: application to mine core characterization, J. Anal. At. Spectrom. 32 (2017) 1527–1534, https://doi.org/10.1039/C7JA00185A.
[153] C. Derrick Quarles, J.J. Gonzalez, L.J. East, J.H. Yoo, M. Morey, R.E. Russo, Fluorine analysis using laser induced breakdown spectroscopy (LIBS), J. Anal. At. Spectrom. 29 (2014) 1238–1242, https://doi.org/10.1039/C4JA00061G.
[154] J.R. Chirinos, D.D. Oropeza, J.J. Gonzalez, H. Hou, M. Morey, V. Zorba, R.E. Russo, Simultaneous 3-dimensional elemental imaging with LIBS and LA-ICP-MS, J. Anal. At. Spectrom. 29 (2014) 1292–1298, https://doi.org/10.1039/C4JA00066H.
[155] T. Xu, J. Liu, Q. Shi, Y. He, G. Niu, Y. Duan, Multi-elemental surface mapping and analysis of carbonaceous shale by laser-induced breakdown spectroscopy, Spectrochim. Acta Part B At. Spectrosc. 115 (2016) 31–39, https://doi.org/10.1016/j.sab.2015.10.008.
[156] J. Jain, C.D. Quarles, J. Moore, D.A. Hartzler, D. McIntyre, D. Crandall, Elemental mapping and geochemical characterization of gas producing shales by laser induced breakdown spectroscopy, Spectrochim. Acta Part B At. Spectrosc. 150 (2018) 1–8, https://doi.org/10.1016/j.sab.2018.09.010.
[157] J.A. Meima, D. Rammlmair, Investigation of compositional variations in chromitite ore with imaging laser induced breakdown spectroscopy and spectral angle mapper classification algorithm, Chem. Geol. 532 (2020), 119376, https://doi.org/10.1016/j.chemgeo.2019.119376.
[158] K. Rifai, L.-Ç. Özcan, F.R. Doucet, K. Rhoderick, F. Vidal, Ultrafast elemental mapping of platinum group elements and mineral identification in platinum-palladium ore using laser induced breakdown spectroscopy, Minerals 10 (2020) 207, https://doi.org/10.3390/min10030207.
[159] J. El Haddad, E.S. de Lima Filho, F. Vanier, A. Harhira, C. Padioleau, M. Sabsabi, G. Wilkie, A. Blouin, Multiphase mineral identification and quantification by laser-induced breakdown spectroscopy, Miner. Eng. 134 (2019) 281–290, https://doi.org/10.1016/j.mineng.2019.02.025.
[160] EU publications, Raw materials scoreboard 2018. https://op.europa.eu/en/publication-detail/-/publication/117c8d9b-e3d3-11e8-b690-01aa75ed71a1, 2018. (Accessed 29 June 2020).
[161] K. Jancsek, P. Janovszky, Gábor Galbács, M.-T. Tivadar, Quantitative determination of lithium in granite rock-forming minerals by laser-induced breakdown spectroscopy (LIBS), in: Book Abstr. Brno, 2019, p. 211. http://libs.ceitec.cz/files/281/213.pdf.
[162] M. Corsi, G. Cristoforetti, V. Palleschi, V. Salvetti, E. Tognoni, Surface compositional mapping of pigments on a roman fresco by CF-LIBS, in: Proc. First Int. Conf. Laser-Induc. Breakdown Appl, 2000, p. 74. Tirrenia, Italy.
[163] R. Grönlund, M. Lundqvist, S. Svanberg, Remote imaging laser-induced breakdown spectroscopy and remote cultural heritage ablative cleaning, Opt. Lett. 30 (2005) 2882–2884, https://doi.org/10.1364/OL.30.002882.
[164] R. Grönlund, M. Lundqvist, S. Svanberg, Remote imaging laser-induced breakdown spectroscopy and laser-induced fluorescence spectroscopy using nanosecond pulses from a mobile lidar system, Appl. Spectrosc. 60 (2006) 853–859, https://doi.org/10.1366/000370206778062138.
[165] F.J. Fortes, J. Cuñat, L.M. Cabalín, J.J. Laserna, In situ analytical assessment and chemical imaging of historical buildings using a man-portable laser system, Appl. Spectrosc. 61 (2007) 558–564, https://doi.org/10.1366/000370207780807722.
[166] L. Bassel, V. Motto-Ros, F. Trichard, F. Pelascini, F. Ammari, R. Chapoulie, C. Ferrier, D. Lacanette, B. Bousquet, Laser-induced breakdown spectroscopy for elemental characterization of calcitic alterations on cave walls, Environ. Sci. Pollut. Res. 24 (2017) 2197–2204, https://doi.org/10.1007/s11356-016-7468-5.
[167] O. Syta, B. Wagner, E. Bulska, D. Zielińska, G.Z. Żukowska, J. Gonzalez, R. Russo, Elemental imaging of heterogeneous inorganic archaeological samples by means of simultaneous laser induced breakdown spectroscopy and laser ablation inductively coupled plasma mass spectrometry measurements, Talanta 179 (2018) 784–791, https://doi.org/10.1016/j.talanta.2017.12.011.
[168] G.S. Senesi, B. Campanella, E. Grifoni, S. Legnaioli, G. Lorenzetti, S. Pagnotta, F. Poggialini, V. Palleschi, O. De Pascale, Elemental and mineralogical imaging of a weathered limestone rock by double-pulse micro-Laser-Induced Breakdown Spectroscopy, Spectrochim. Acta Part B At. Spectrosc. 143 (2018) 91–97, https://doi.org/10.1016/j.sab.2018.02.018.
[169] M. Hoehse, A. Paul, I. Gornushkin, U. Panne, Multivariate classification of pigments and inks using combined Raman spectroscopy and LIBS, Anal. Bioanal. Chem. 402 (2012) 1443–1450, https://doi.org/10.1007/s00216-011-5287-6.
[170] A. Giakoumaki, K. Melessanaki, D. Anglos, Laser-induced breakdown spectroscopy (LIBS) in archaeological science—applications and prospects, Anal. Bioanal. Chem. 387 (2007) 749–760, https://doi.org/10.1007/s00216-006-0908-1.
[171] H. Bette, R. Noll, G. Müller, H.-W. Jansen, Ç. Nazikkol, H. Mittelstädt, High-speed scanning laser-induced breakdown spectroscopy at 1000 Hz with single pulse evaluation for the detection of inclusions in steel, J. Laser Appl. 17 (2005) 183–190, https://doi.org/10.2351/1.1961738.
[172] R.R.V. Carvalho, J.A.O. Coelho, J.M. Santos, F.W.B. Aquino, R.L. Carneiro, E.R. Pereira-Filho, Laser-induced breakdown spectroscopy (LIBS) combined with hyperspectral imaging for the evaluation of printed circuit board composition, Talanta 134 (2015) 278–283, https://doi.org/10.1016/j.talanta.2014.11.019.
[173] C.M. Ahamer, K.M. Riepl, N. Huber, J.D. Pedarnig, Femtosecond laser-induced breakdown spectroscopy: elemental imaging of thin films with high spatial resolution, Spectrochim. Acta Part B At. Spectrosc. 136 (2017) 56–65, https://doi.org/10.1016/j.sab.2017.08.005.
[174] V.N. Lednev, P.A. Sdvizhenskii, M.Y. Grishin, V.V. Cheverikin, A.Y. Stavertiy, R.S. Tretyakov, M.V. Taksanc, S.M. Pershin, Laser-induced breakdown spectroscopy for three-dimensional elemental mapping of composite materials synthesized by additive technologies, Appl. Optic. 56 (2017) 9698–9705, https://doi.org/10.1364/AO.56.009698.
[175] P. Lucena, J.M. Vadillo, J.J. Laserna, Mapping of platinum group metals in automotive exhaust three-way catalysts using laser-induced breakdown spectrometry, Anal. Chem. 71 (1999) 4385–4391, https://doi.org/10.1021/ac9902998.
[176] F. Trichard, L. Sorbier, S. Moncayo, Y. Blouët, C.-P. Lienemann, V. Motto-Ros, Quantitative elemental imaging of heterogeneous catalysts using laser-induced breakdown spectroscopy, Spectrochim. Acta Part B At. Spectrosc. 133 (2017) 45–51, https://doi.org/10.1016/j.sab.2017.04.008.
[177] F. Trichard, F. Gaulier, J. Barbier, D. Espinat, B. Guichard, C.-P. Lienemann, L. Sorbier, P. Levitz, V. Motto-Ros, Imaging of alumina supports by laser-induced breakdown spectroscopy: a new tool to understand the diffusion of trace metal impurities, J. Catal. 363 (2018) 183–190, https://doi.org/10.1016/j.jcat.2018.04.013.
[178] H. Hou, L. Cheng, T. Richardson, G. Chen, M. Doeff, R. Zheng, R. Russo, V. Zorba, Three-dimensional elemental imaging of Li-ion solid-state electrolytes using fs-laser induced breakdown spectroscopy (LIBS), J. Anal. At. Spectrom. 30 (2015) 2295–2302, https://doi.org/10.1039/C5JA00250H.
[179] D. Rettenwander, R. Wagner, A. Reyer, M. Bonta, L. Cheng, M.M. Doeff, A. Limbeck, M. Wilkening, G. Amthauer, Interface instability of Fe-stabilized Li7La3Zr2O12 versus Li metal, J. Phys. Chem. C Nanomater. Interfaces. 122 (2018) 3780–3785, https://doi.org/10.1021/acs.jpcc.7b12387.
[180] S. Imashuku, H. Taguchi, T. Kawamata, S. Fujieda, S. Kashiwakura, S. Suzuki, K. Wagatsuma, Quantitative lithium mapping of lithium-ion battery cathode using laser-induced breakdown spectroscopy, J. Power Sources 399 (2018) 186–191, https://doi.org/10.1016/j.jpowsour.2018.07.088.
[181] C. Gottlieb, S. Millar, S. Grothe, G. Wilsch, 2D evaluation of spectral LIBS data derived from heterogeneous materials using cluster algorithm, Spectrochim. Acta Part B At. Spectrosc. 134 (2017) 58–68, https://doi.org/10.1016/j.sab.2017.06.005.
[182] C. Li, X. Wu, C. Zhang, H. Ding, J. Hu, G.-N. Luo, In situ chemical imaging of lithiated tungsten using laser-induced breakdown spectroscopy, J. Nucl. Mater. 452 (2014) 10–15, https://doi.org/10.1016/j.jnucmat.2014.04.041.
[183] R. Hai, C. Li, H. Wang, H. Ding, H. Zhuo, J. Wu, G.-N. Luo, Characterization of Li deposition on the first wall of EAST using laser-induced breakdown spectroscopy, J. Nucl. Mater. 438 (2013) S1168–S1171, https://doi.org/10.1016/j.jnucmat.2013.01.258.
[184] X. Wang, V. Motto-Ros, G. Panczer, D. De Ligny, J. Yu, J.M. Benoit, J.L. Dussossoy, S. Peuget, Mapping of rare earth elements in nuclear waste glass–ceramic using micro laser-induced breakdown spectroscopy, Spectrochim. Acta Part B At. Spectrosc. 87 (2013) 139–146, https://doi.org/10.1016/j.sab.2013.05.022.
[185] M. López-López, C. Alvarez-Llamas, J. Pisonero, C. García-Ruiz, N. Bordel, An exploratory study of the potential of LIBS for visualizing gunshot residue patterns, Forensic Sci. Int. 273 (2017) 124–131, https://doi.org/10.1016/j.forsciint.2017.02.012.
[186] L. Zou, B. Kassim, J.P. Smith, J.D. Ormes, Y. Liu, Q. Tu, X. Bu, In situ analytical characterization and chemical imaging of tablet coatings using laser induced breakdown spectroscopy (LIBS), Analyst 143 (2018) 5000–5007, https://doi.org/10.1039/C8AN01262H.
[187] J.P. Smith, L. Zou, Y. Liu, X. Bu, Investigation of minor elemental species within tablets using in situ depth profiling via laser-induced breakdown spectroscopy hyperspectral imaging, Spectrochim. Acta Part B At. Spectrosc. 165 (2020), 105769, https://doi.org/10.1016/j.sab.2020.105769.
[188] S.-H. Lee, J.-H. Choi, J.-H. In, S. Jeong, Fast compositional mapping of solar cell by laser spectroscopy technique for process monitoring, Int. J. Precis. Eng. Manuf.-Green Technol. 6 (2019) 189–196, https://doi.org/10.1007/s40684-019-00083-8.
[189] P. Veber, K. Bartosiewicz, J. Debray, G. Alombert-Goget, O. Benamara, V. Motto-Ros, M.P. Thi, A. Borta-Boyon, H. Cabane, K. Lebbou, F. Levassort, K. Kamada, A. Yoshikawa, M. Maglione, Lead-free piezoelectric crystals grown by the micro-pulling down technique in the BaTiO3–CaTiO3–BaZrO3 system, CrystEngComm 21 (2019) 3844–3853, https://doi.org/10.1039/C9CE00405J.
[190] D. Prochazka, P. Pořízka, J. Novotný, A. Hrdlička, K. Novotný, P. Šperka, J. Kaiser, Triple-pulse LIBS: laser-induced breakdown spectroscopy signal enhancement by combination of pre-ablation and re-heating laser pulses,

J. Anal. At. Spectrom. 35 (2020) 293–300, https://doi.org/10.1039/C9JA00323A.
[191] D.V. S, S.D. George, V.B. Kartha, S. Chidangil, U.V. K, Hybrid LIBS-Raman-LIF systems for multi-modal spectroscopic applications: a topical review, Appl. Spectrosc. Rev. (2020) 1–29, https://doi.org/10.1080/05704928.2020.1800486, 0.
[192] K.M.M. Shameem, K.S. Choudhari, A. Bankapur, S.D. Kulkarni, V.K. Unnikrishnan, S.D. George, V.B. Kartha, C. Santhosh, A hybrid LIBS–Raman system combined with chemometrics: an efficient tool for plastic identification and sorting, Anal. Bioanal. Chem. 409 (2017) 3299–3308, https://doi.org/10.1007/s00216-017-0268-z.
[193] M. Hoehse, A. Paul, I. Gornushkin, U. Panne, Multivariate classification of pigments and inks using combined Raman spectroscopy and LIBS, Anal. Bioanal. Chem. 402 (2012) 1443–1450, https://doi.org/10.1007/s00216-011-5287-6.

Andreas Limbeck is an expert in the field of atomic spectroscopy with more than 15 years' experience in the development of advanced analytical procedures for the reliable determination of inorganic components in a wide range of technological, environmental as well as biological samples. In the last years, he developed advanced expertise in the application of the laser-based techniques LA-ICP-MS and LIBS for the spatially resolved chemical analysis of solid materials, in particular for the quantitative determination of elemental distributions in various materials. Since 2015 he is associate professor at the Faculty of Technical Chemistry at TU Wien.

Lukas Brunnbauer, MSc received his BSc and MSc in Technical Chemistry from the TU Wien. Currently he is doing his PhD at TU Wien in the research group "Surface Analytics, Trace Analytics and Chemometry" headed by Assoc. Prof. Dr. Andreas Limbeck in cooperation with Infineon Austria AG. His research is mainly focused on polymer analysis using a tandem LA-ICP-MS/LIBS setup.

Hans Lohninger is working at the Institute of Chemical Technologies and Analytics at Technische Universität Wien. He holds an MSc from the University of Vienna and a PhD from the TU Wien. His interests currently focus on hyperspectral imaging (HSI) and the combination of chemometrics with HSI. He has developed many applications of HSI in a wide range of fields, covering spectroscopic techniques such as MS, SIMS, infrared, Raman, UVVIS, LIBS, EDX and THz. Besides his academic obligations he is running a small software development company which provides both custom-specific solutions to chemometric problems and general-purpose software for hyperspectral imaging.

Pavel Porizka studied physics and nanotechnology at the Brno University of Technology (BUT) in Brno, Czech Republic where he received a Ph.D. degree in 2014. Considering scientific internships, he joined Federal Institute for Materials Research and Testing in Berlin, DE and later he was a Fulbright postdoc fellow at the University of Florida in Gainesville, US-FL. Currently, he is a postdoc and the leader of Laser spectroscopy laboratory at CEITEC BUT and an associate professor at the Faculty of Mechanical Engineering BUT. His main research interest ranges from machine learning through industrial to bio-applications of laser spectroscopic techniques.

Pavlína Modlitbová is a postdoc in Laser spectroscopy laboratory at CEITEC BUT, who achieved her PhD degree in 2016 at Faculty of Chemistry BUT in the field of terrestrial nanoecotoxicology. As a PhD student she was a trainee at the Zoology department at University of Ljubljana for eight months. Since then, she personally focus on using laser spectroscopy in the analysis of biological samples especially in the detection of various trace elements, new xenobiotics as nanoparticles (Cd-based, gold, and photon upconversion NPs) or microplastics in plants. Her main research interest is in various bio-applications of LIBS.

Jozef Kaiser received his Ph.D. at the Faculty of Mechanical Engineering, Brno University of Technology (BUT) in 2001 and was promoted to a full professor in 2013. He has an extensive experience in laser spectroscopy and computed tomography when dealing more than 20 years with the state-of-the-art and cooperating with world-renowned laboratories, such as Synchrotron Elettra in Trieste, IT, Oak Ridge National Laboratory in Oak Ridge, US-TN and the University of Tokushima in Tokushima, JP. In 2013, he established and leads a research group Materials Characterization and Advanced Coatings at CEITEC BUT. Since then, he founded four technological start-ups.

Patrick Janovszky received his B.Sc. and later M.Sc. degrees in Chemistry from the University of Szeged, Hungary. He is currently working on his PhD thesis at the same university under the supervision of Prof. G. Galbács on LIBS and LA-ICP-MS method development for the multielemental analysis of environmental samples. His professional experience includes the trace elemental and isotope ratio analysis of biological, geological and plant samples by various spectroscopy techniques.

Albert Kéri received his B.Sc. in Environmental Engineering (2014) and his M.Sc. in Chemistry (2016) from the University of Szeged, Hungary. The topic of his PhD thesis – that he defended in 2020 at the University of Szeged – was ICP-MS based analytical method development for the investigation of multi-component nanoparticles. He participated in several national and European founded research and R + D projects where he developed ICP-MS and LIBS based analytical methods. Currently he is a postdoctoral researcher at the Inorganic and Analytical Chemistry Department at University of Szeged.

Gábor Galbács is holding MSc diplomas in chemistry and physics, as well as in environmental sciences (University of Szeged, Hungary). He obtained a PhD/CSc degree from the same university in 1998 and a DSc title from the Hungarian Academy of Sciences in 2013, both in the field of analytical chemistry. His research is diverse, but focuses on fundamental studies and instrumentation/method development for laser and plasma analytical spectroscopy, mostly LIBS, ICP-MS and ICP-AES. He is a full professor and the head of the Department of Inorganic and Analytical Chemistry at the University of Szeged since 2014.